

# ***MIKE* High Resolution Observation and Raman-scattering by Atomic Hydrogen in the Symbiotic Nova RR Telescopii**

**Jeong-Eun Heo<sup>1</sup>, Hee-Won Lee<sup>1</sup>, Rodolfo Angeloni<sup>2</sup>, Tali Palma<sup>3</sup>, Francesco Di Miile<sup>4</sup>**

<sup>1</sup> Sejong University, Korea

<sup>2</sup> Universidad de La Serena, Chile

<sup>3</sup> Observatorio Astronómica, Argentina

<sup>4</sup> Las Campanas Observatory, Chile



**세종대학교**  
SEJONG UNIVERSITY



Área de Astronomía  
Departamento de Física y Astronomía - Universidad de La Serena



**한국천문연구원**  
Korea Astronomy & Space Science Institute

## I. Introduction

- [C II] 158  $\mu\text{m}$
- C II 1036, 1037 Doublet
- Raman-Scattered C II Lines

## II. Observation

- RR Tel
- MIKE Spectroscopy
- Raman Lines in RR Tel

## III. Raman C II and ISM

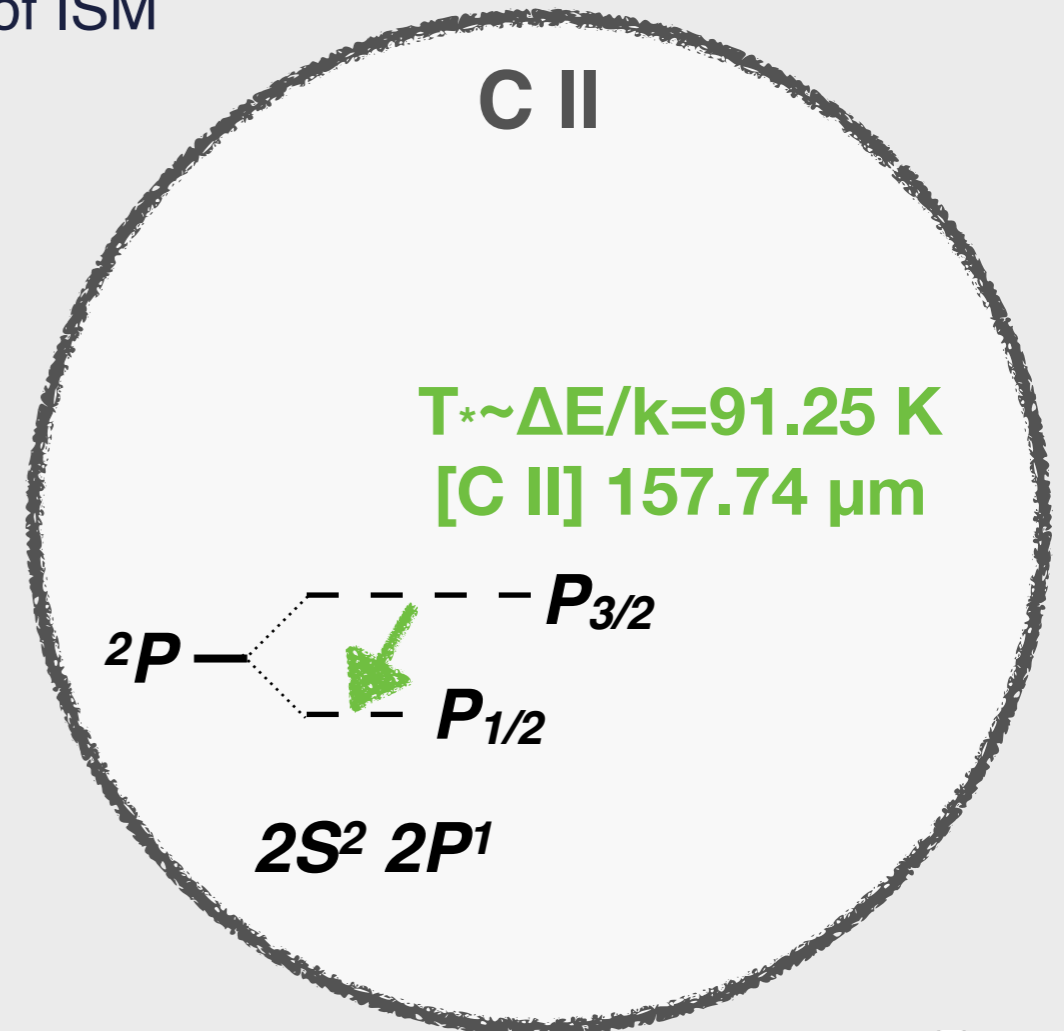
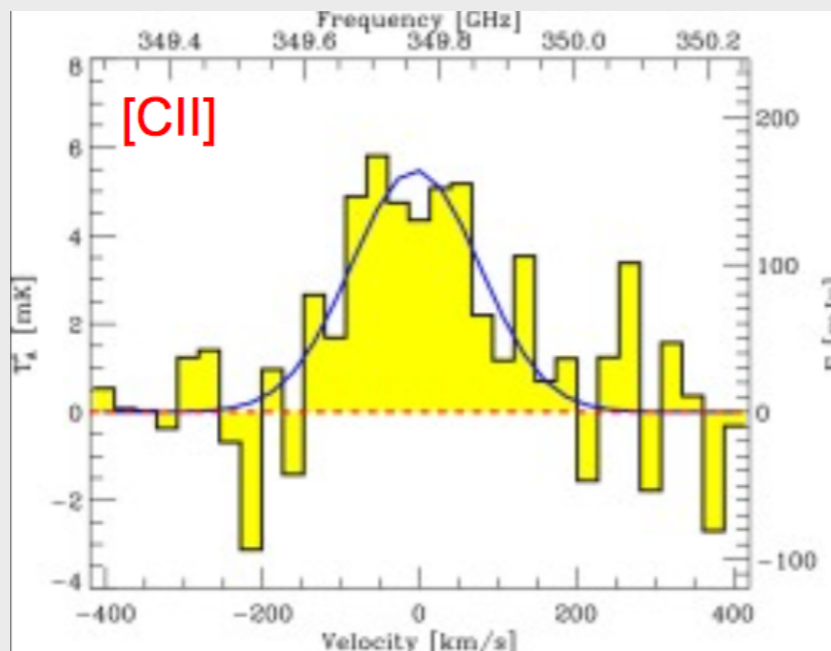
- Incident C II 1036, 1037 Emissions
- C II 1335 Triplet
- Optical Depth of C II Emissions
- Extinction of ISM

## IV. Summary and Discussion

# I. Introduction

## ✓ [C II] 158 $\mu\text{m}$ and ISM

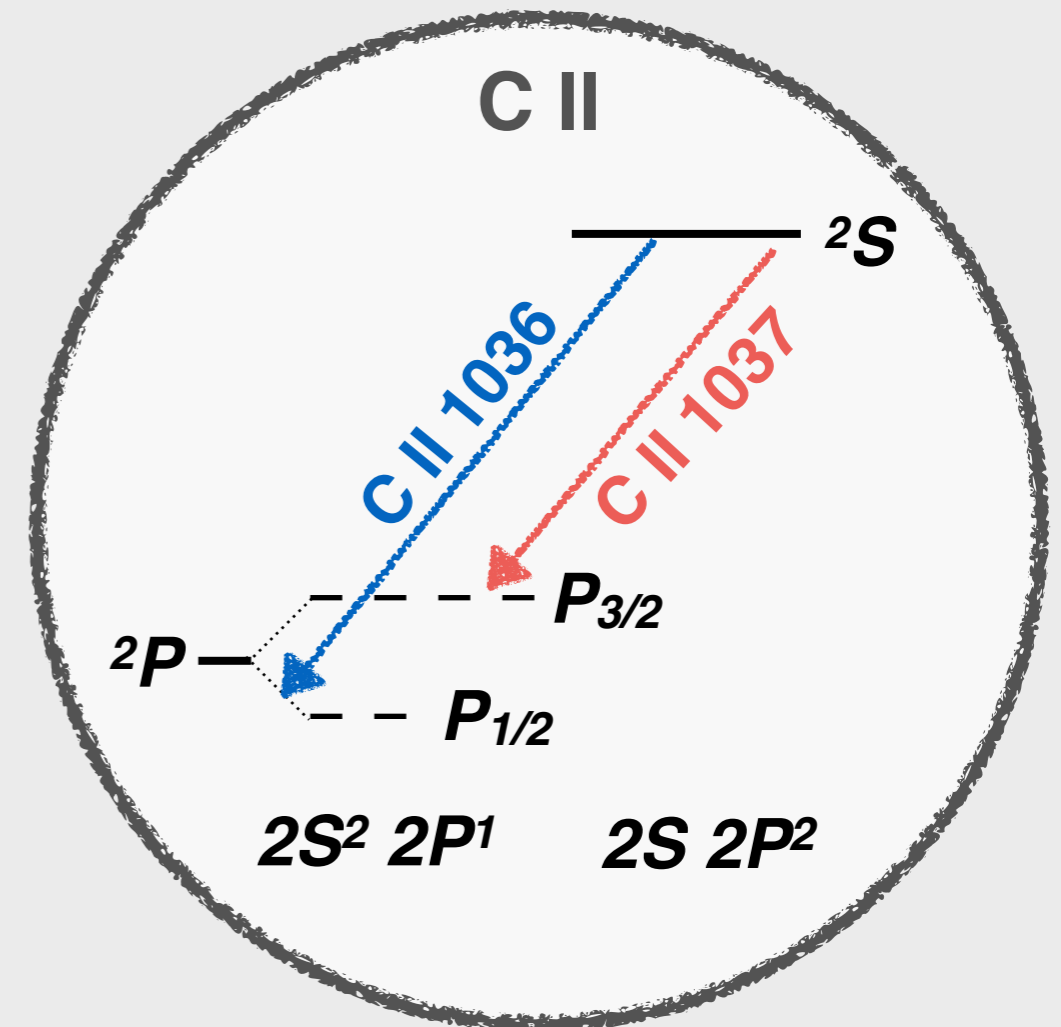
- $2P_{3/2} - 2P_{1/2}$  : **157.74  $\mu\text{m}$**
- In cold regions, cooling is dominated by collisional excitation of C+ by collisions with other particles (e.g, H or free electrons and protons).
- An efficient and dominating coolant for neutral gas
- Powerful spectral diagnostics of ISM



# I. Introduction

## ✓ C II 1036, 1037 Doublet

- $2S\ 2P^2\ ^2S_{1/2} - 2S^2\ 2P^1\ ^2P^0_{1/2}$ : **1036.337 Å**
- $2S\ 2P^2\ ^2S_{1/2} - 2S^2\ 2P^1\ ^2P^0_{3/2}$ : **1037.018 Å**



★ INTRODUCTION

🔭 OBSERVATION

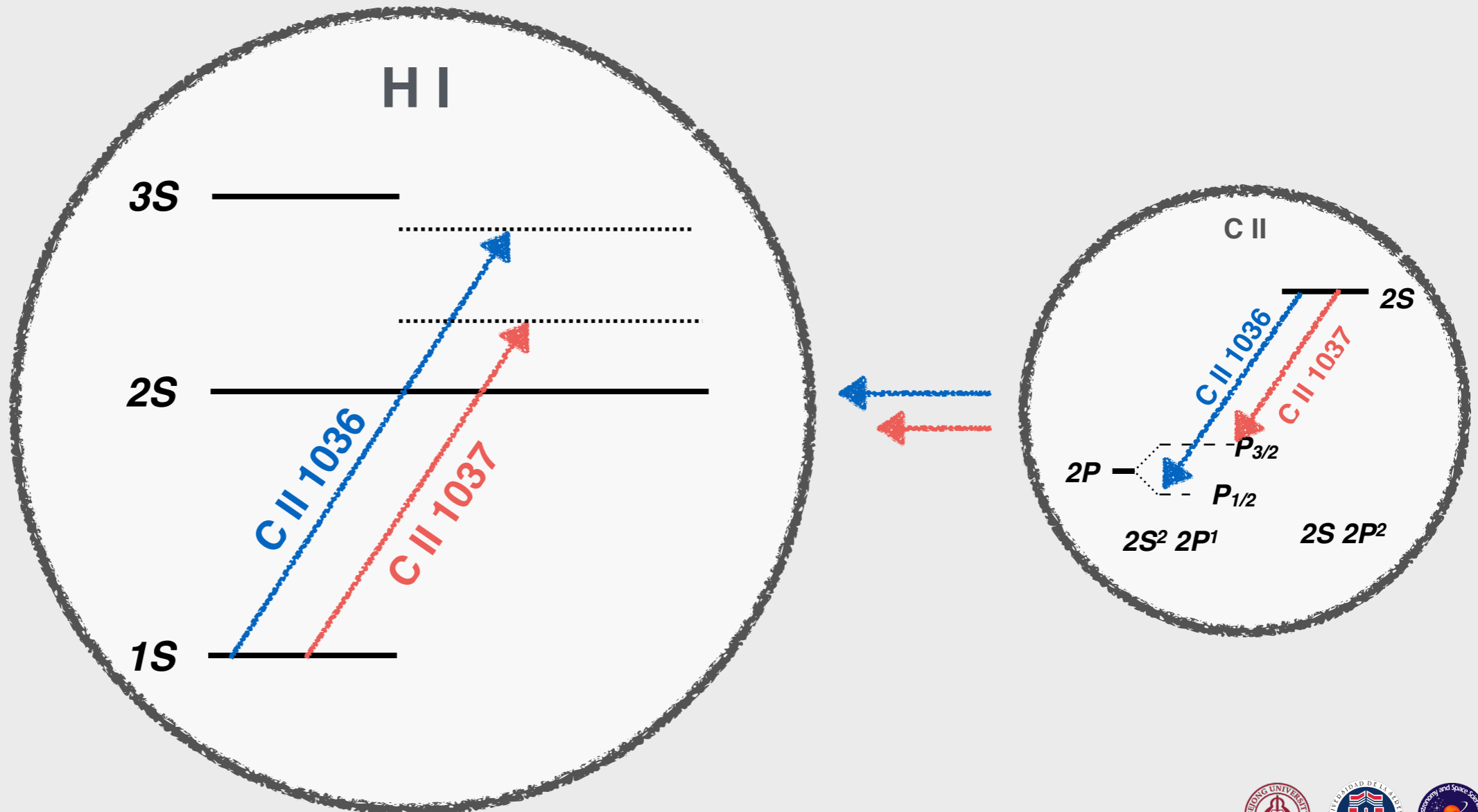
🖥️ SIMULATION

🍺 DISCUSSION

# I. Introduction

## ✓ C II 1036, 1037 Doublet

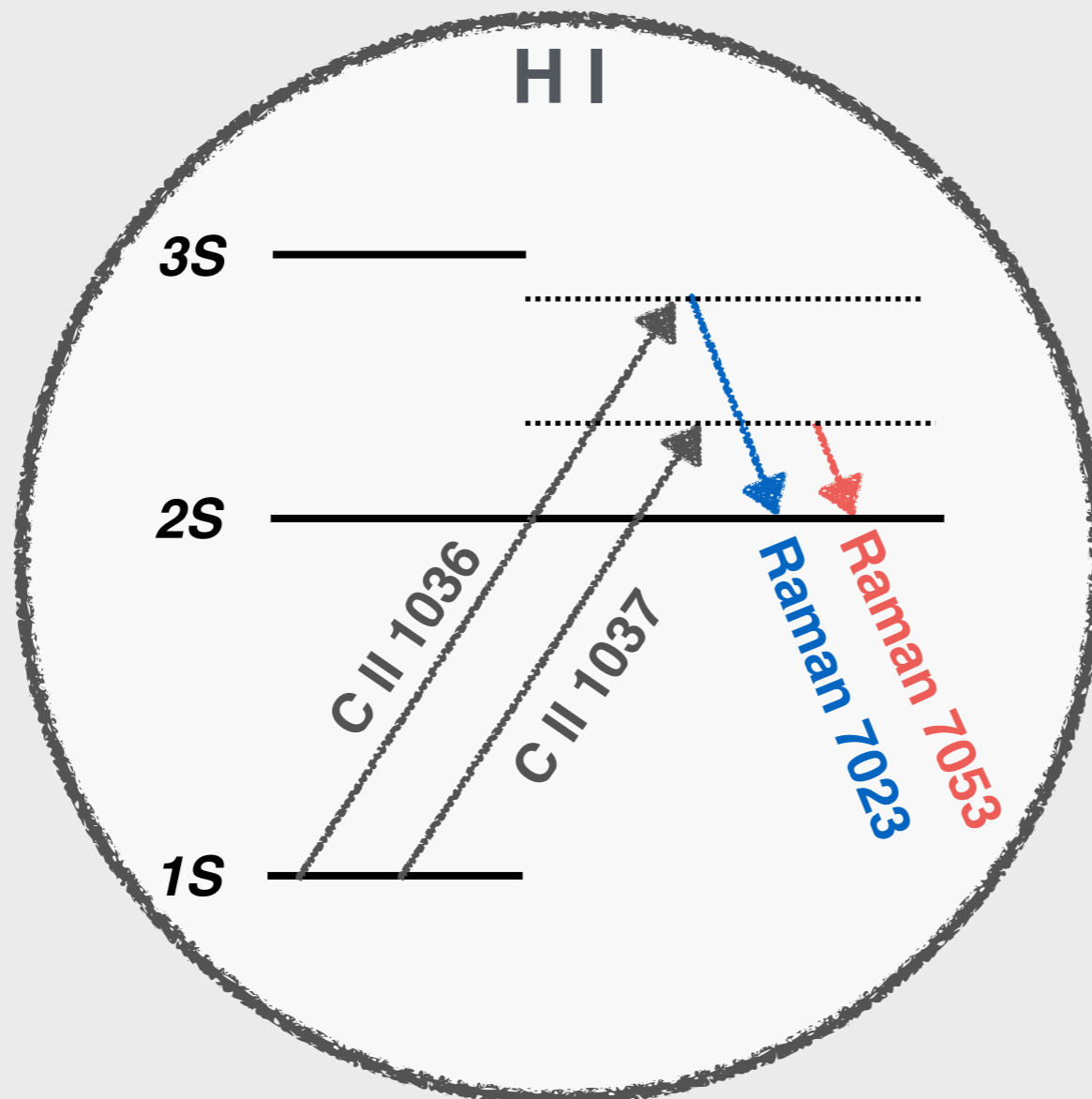
- The C II 1036, 1037 photons are incident on H I in the ground state to excite them in an intermediate level.



# I. Introduction

## ✓ Raman-scattered C II Lines

- The H I de-excite to 2S level with re-emission of an optical photon with center wavelength at 7025 and 7052, respectively.
- **C II 1036** → Raman scattering by H I → **Raman C II at 7023.24 Å**
- **C II 1037** → Raman scattering by H I → **Raman C II at 7053.30 Å**



# I. Introduction

## ✓ Raman-scattered C II Lines

- Only detected in the symbiotic nova V1016 Cyg (Schild & Schmid, 1996)

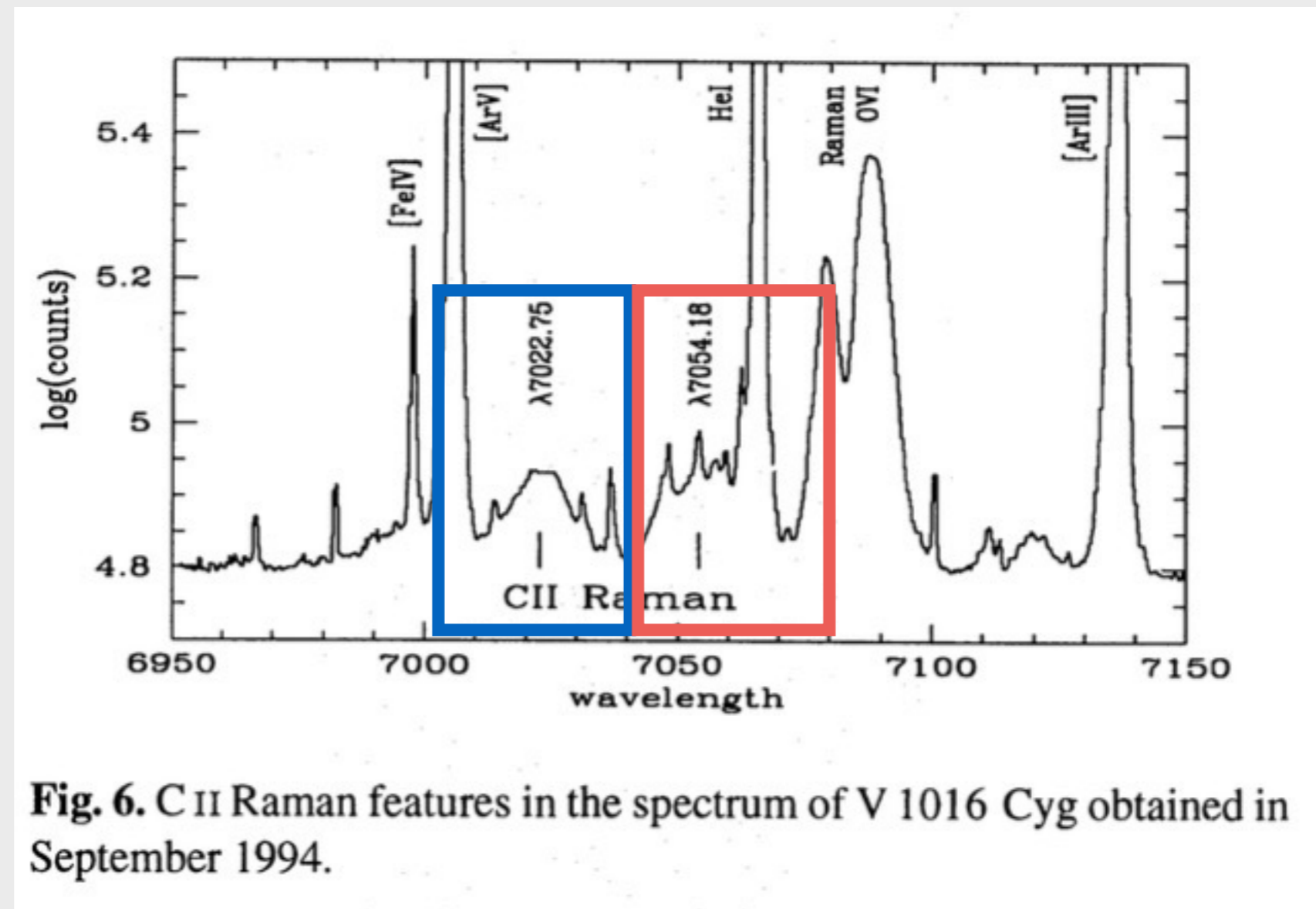
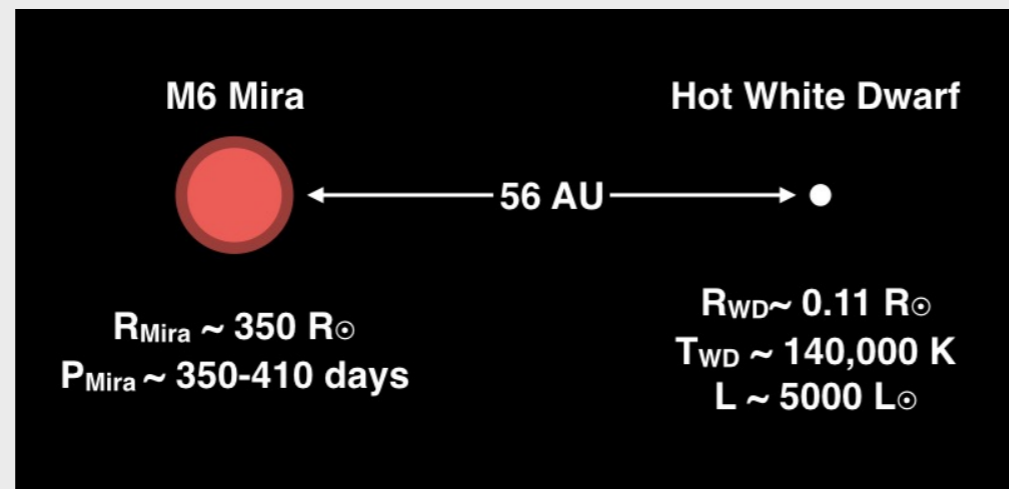


**Fig. 6.** C II Raman features in the spectrum of V 1016 Cyg obtained in September 1994.

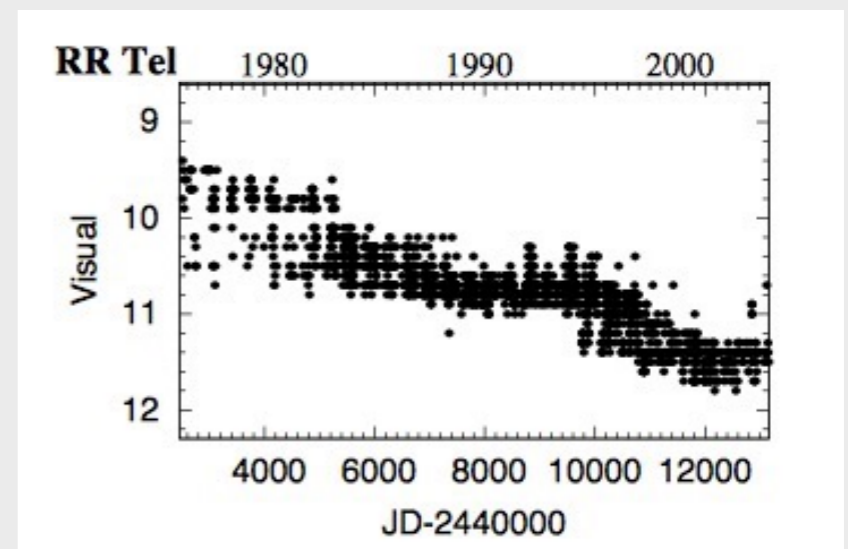
# II. Observation

## ✓ RR Telescopii

- D(Dusty)-type symbiotic nova consisting of a Mira variable and a white dwarf (Whitelock 2003)
- After a nova-like outburst in 1944, its brightness is slowly fading from its peak  $V \sim 7$  mag in 1946 to  $V \sim 11.5$  mag in 2017.
- Distance  $\sim 2.6$  kpc (Schmid & Schild 2002)



Basic Parameters for RR Tel  
 (Feast et al. 1983; Mürset & Schmid 1999; Gromadzki et al. 2009)



Gromadzki et al. (2009)



## II. Observation

★ INTRODUCTION

🔭 OBSERVATION

🖥️ SIMULATION

🗣️ DISCUSSION

### ✓ *MIKE* High Resolution Spectroscopy

- The Magellan Inamori Kyocera Echelle (MIKE)
- 6.5m Clay Telescope, Las Campanas Observatory, Chile
- Spectral Coverage: (Blue) 3,350~5,000 Å (Red) 4,900~9,500 Å
- Resolving Power (Blue)  $R \sim 27,000$  (Red)  $R \sim 35,500$
- Observing Date: 30, July, 2016
- Exposure Time: 2000 sec



# II. Observation

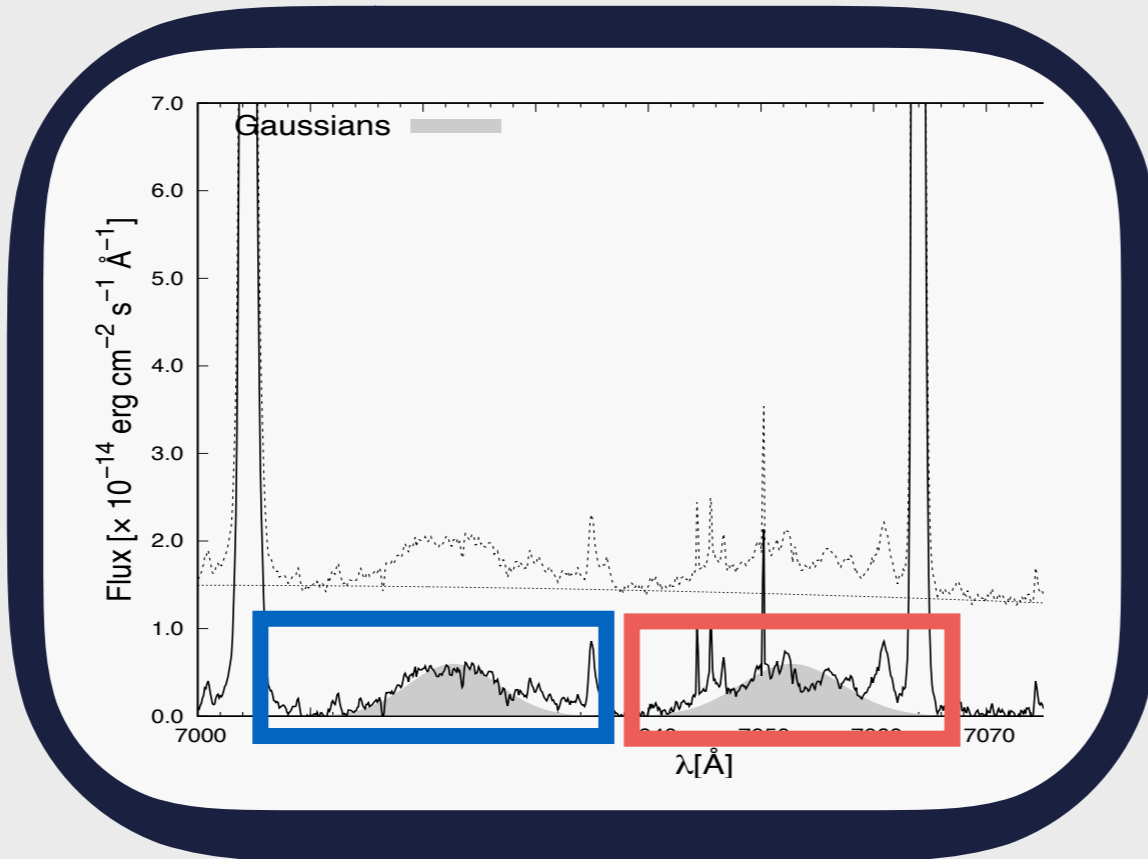
## ✓ Raman-scattered C II Lines in RR Tel

★ INTRODUCTION

 OBSERVATION

 SIMULATION

 DISCUSSION



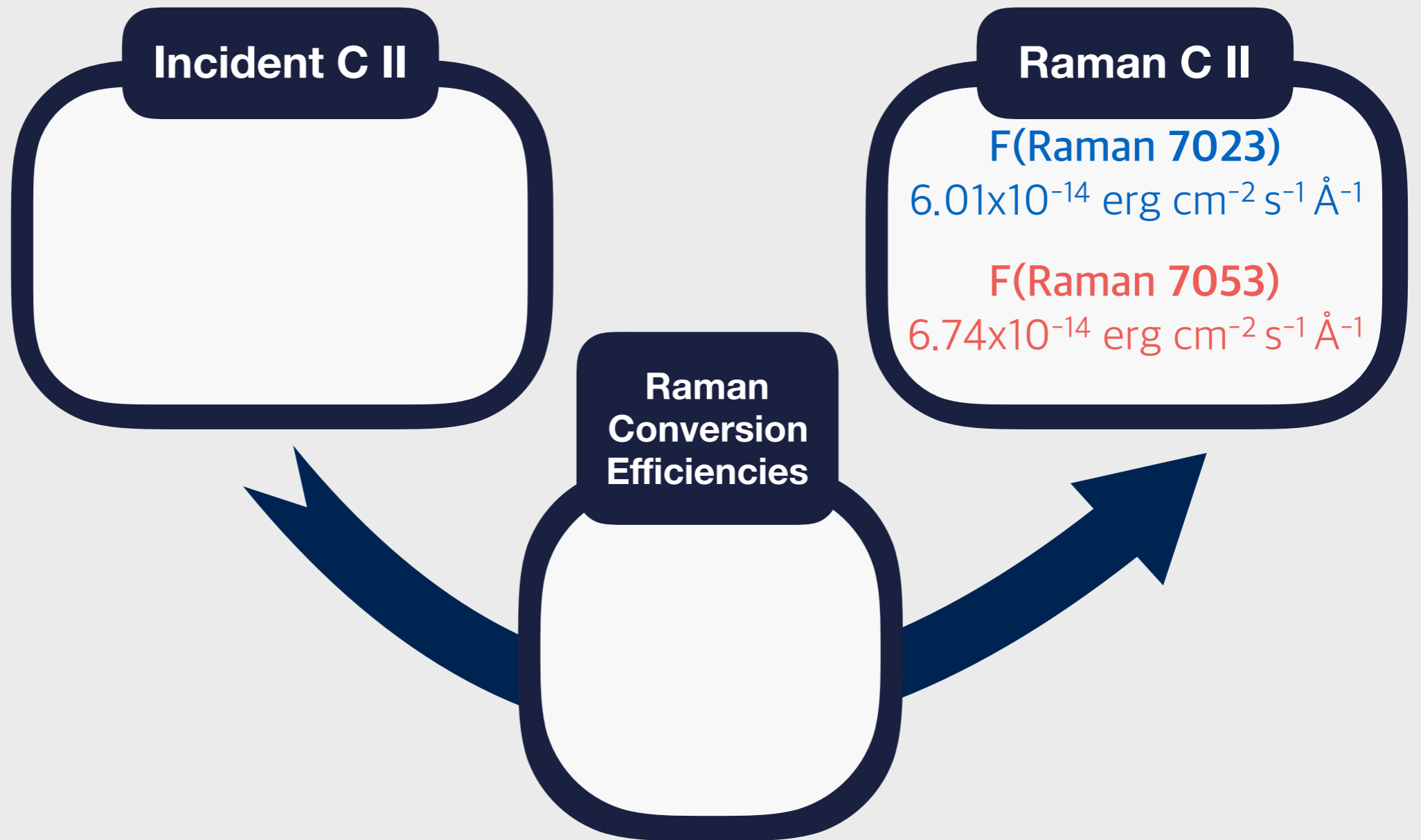
**Raman C II**

**F(Raman 7023)**  
 $6.01 \times 10^{-14} \text{ erg cm}^{-2} \text{ s}^{-1} \text{ \AA}^{-1}$

**F(Raman 7053)**  
 $6.74 \times 10^{-14} \text{ erg cm}^{-2} \text{ s}^{-1} \text{ \AA}^{-1}$

# III. Raman C II and ISM

## ✓ Incident Far-UV C II 1036,1037 Emissions



★ INTRODUCTION

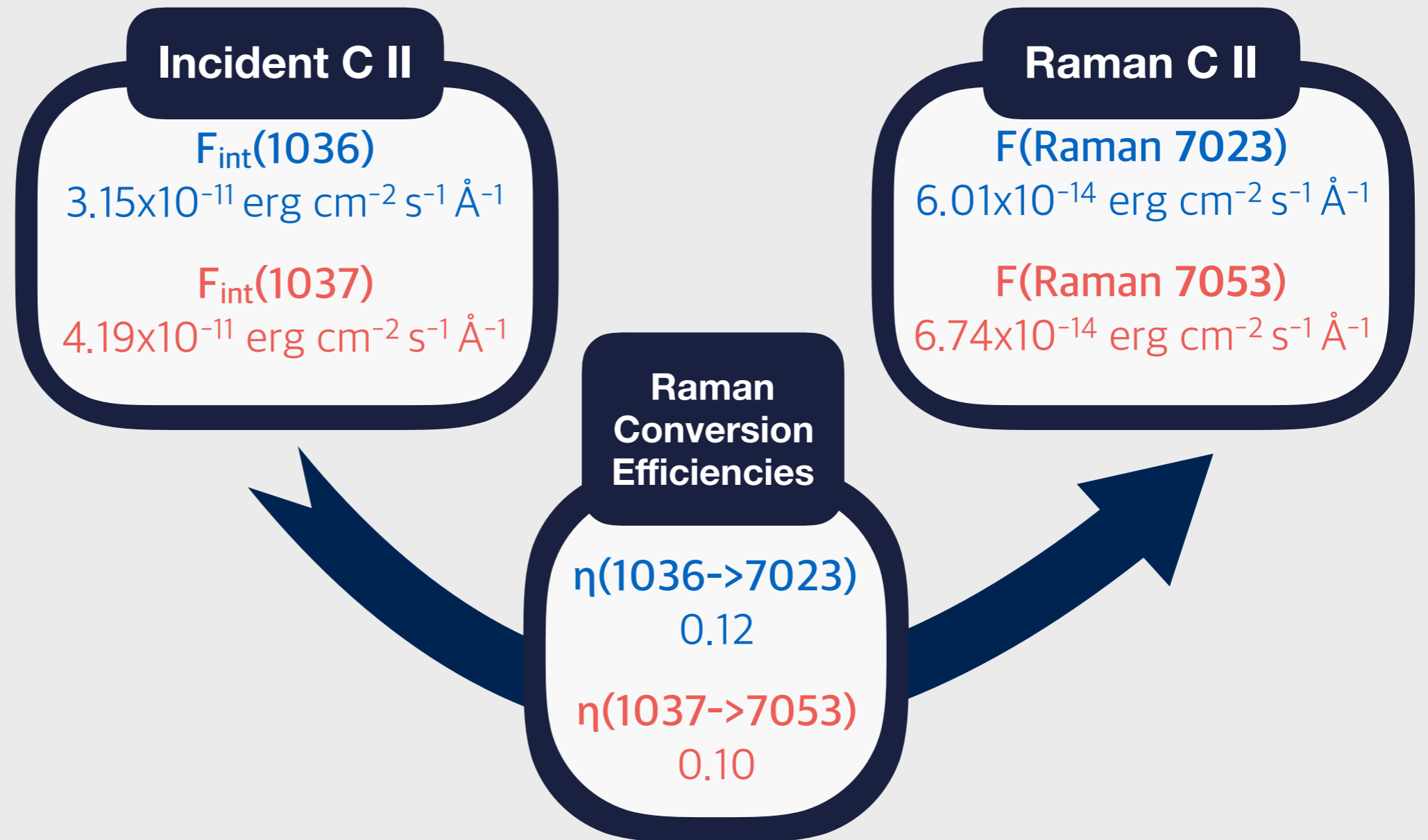
🔭 OBSERVATION

🖥️ SIMULATION

🍺 DISCUSSION

# III. Raman C II and ISM

## ✓ Incident Far-UV C II 1036,1037 Emissions



★ INTRODUCTION

🔭 OBSERVATION

🖥️ SIMULATION

🗣️ DISCUSSION

# III. Raman C II and ISM

## ✓ Comparison with FUSE data

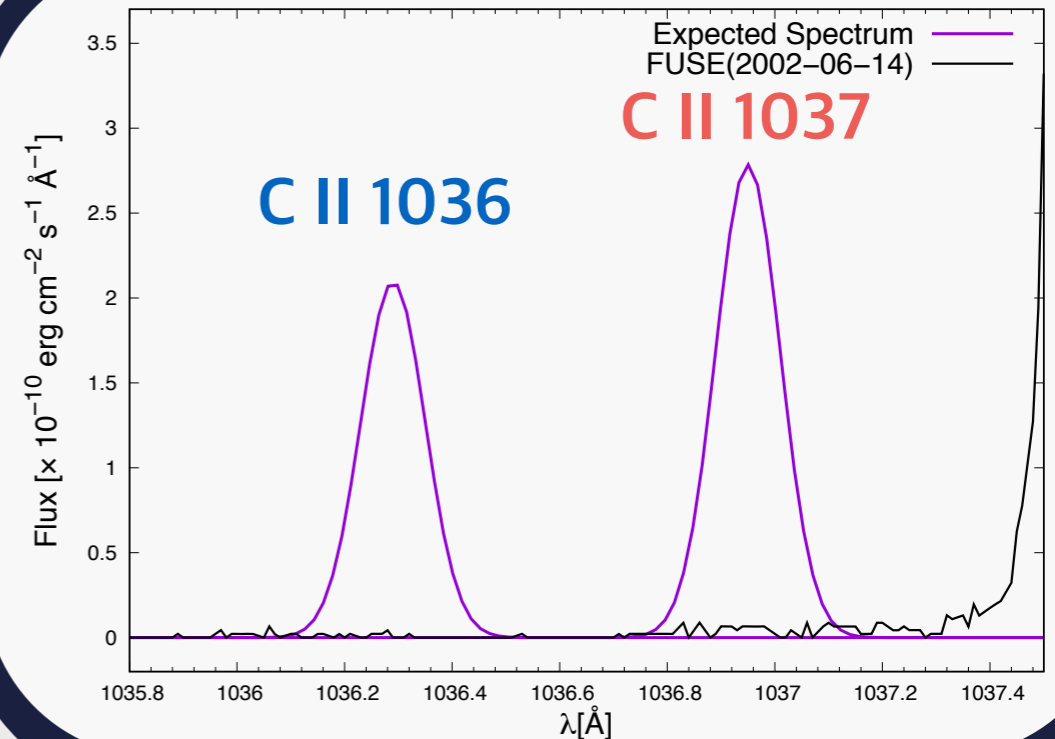
### Incident C II

$F_{\text{int}}(1036)$

$3.15 \times 10^{-11} \text{ erg cm}^{-2} \text{ s}^{-1} \text{ \AA}^{-1}$

$F_{\text{int}}(1037)$

$4.19 \times 10^{-11} \text{ erg cm}^{-2} \text{ s}^{-1} \text{ \AA}^{-1}$



- ✓ A significant amount of C II 1036 and 1037 Å emissions are expected, however they are clearly absent in FUSE data.

# III. Raman C II and ISM

## ✓ C II 1335 Multiplet in IUE Spectrum

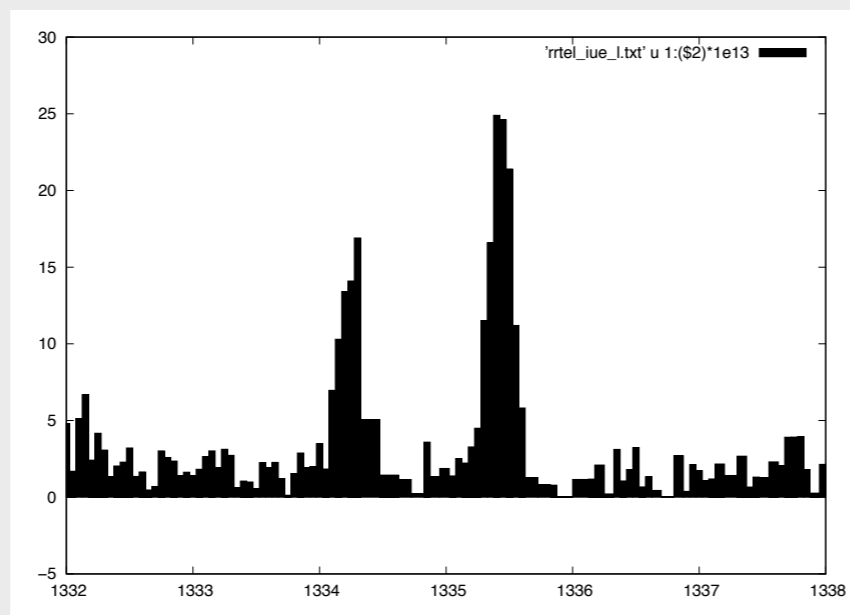
-  $2s2p^2 \ ^2D - 2s^22p \ ^2P^0$ : **1334.53, 1335.66 and 1335.71 Å**

★ INTRODUCTION

🔭 OBSERVATION

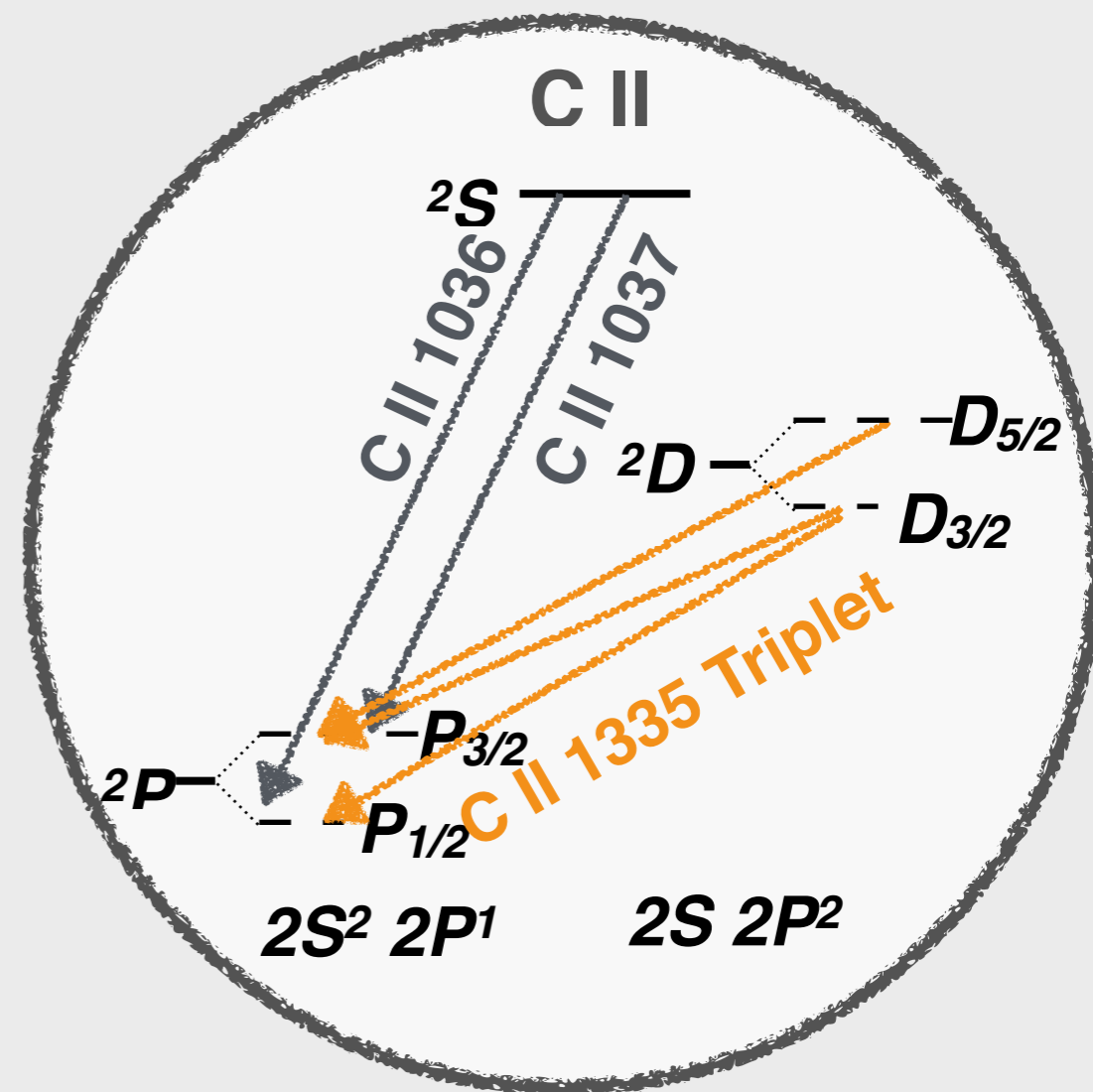
🖥️ SIMULATION

🍺 DISCUSSION



$$F_{\text{obs}}(1335) = 4.43 \times 10^{-13} \text{ erg cm}^{-2} \text{ s}^{-1} \text{ \AA}^{-1}$$

$$F_{\text{obs}}(1336) = 7.15 \times 10^{-13} \text{ erg cm}^{-2} \text{ s}^{-1} \text{ \AA}^{-1}$$



# III. Raman C II and ISM

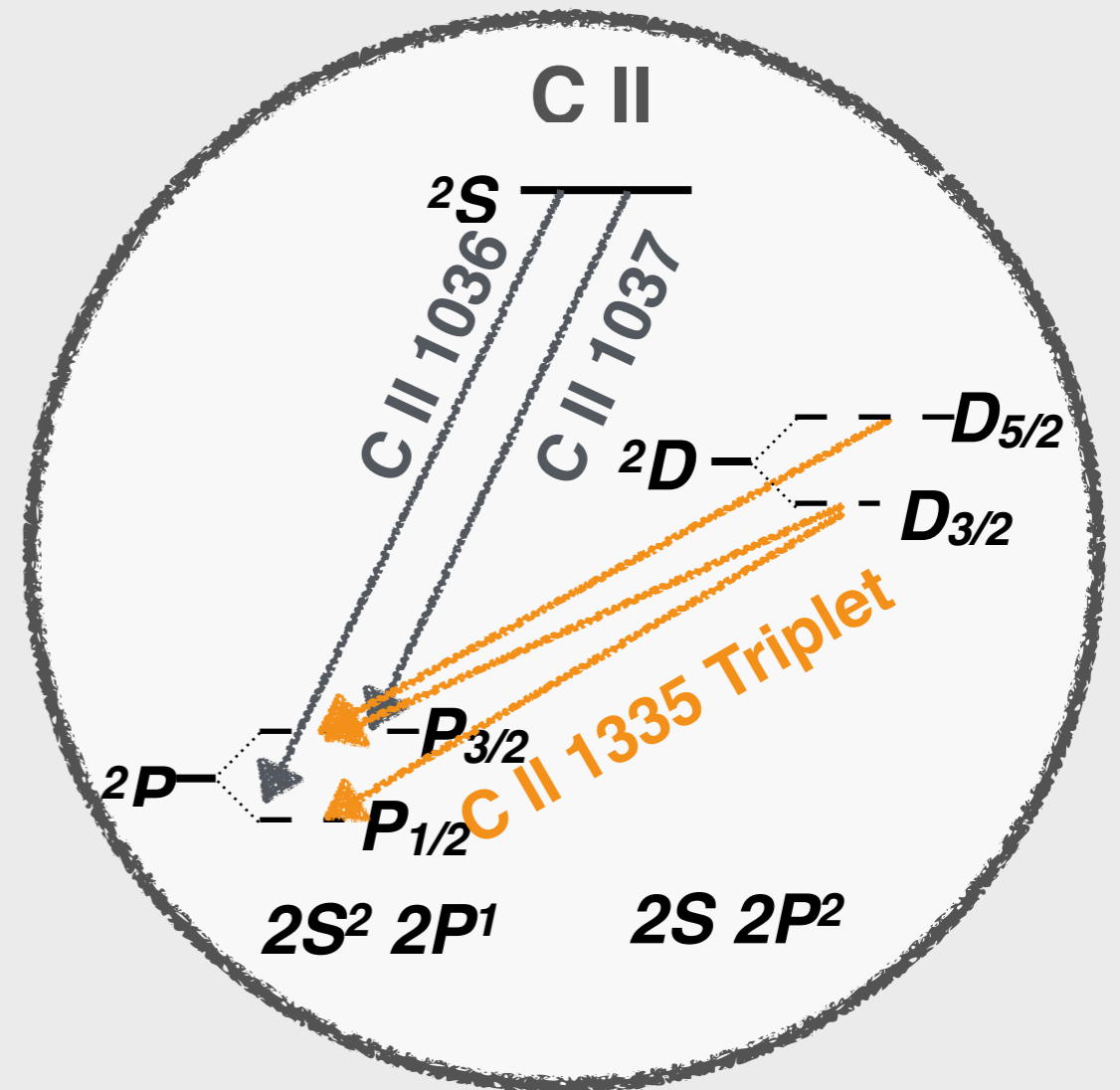
## ✓ C II 1335 Multiplet

-  $2s2p^2 \ ^2D - 2s^22p \ ^2P^0$ : **1334.53, 1335.66 and 1335.71Å**

$$F_{ij} = F_{ik} \times \frac{\Upsilon_{ij}}{\Upsilon_{ik}}$$

$$F_{\text{int}}(1335) = F_{\text{int}}(1036) \times \Upsilon_{1335}/\Upsilon_{1036}$$

$$F_{\text{int}}(1336) = F_{\text{int}}(1037) \times \Upsilon_{1336}/\Upsilon_{1037}$$



★ INTRODUCTION

🔭 OBSERVATION

🖥️ SIMULATION

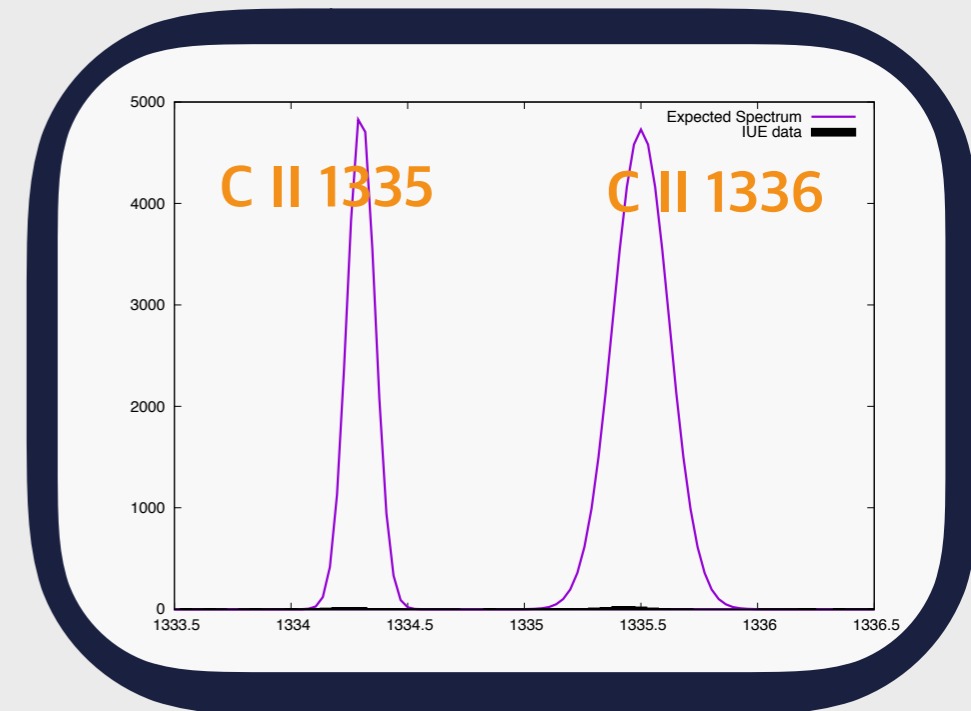
🍺 DISCUSSION

# III. Raman C II and ISM

## ✓ C II 1335 Multiplet in IUE Spectrum

-  $2s2p^2 \ ^2D - 2s^22p \ ^2P^0$ : **1334.53, 1335.66 and 1335.71 Å**

$$F_{ij} = F_{ik} \times \frac{\Upsilon_{ij}}{\Upsilon_{ik}}$$



$$F_{\text{int}}(1335) = F_{\text{int}}(1036) \times \Upsilon_{1335}/\Upsilon_{1036}$$

$$7.41 \times 10^{-11} \text{ erg cm}^{-2} \text{ s}^{-1} \text{ \AA}^{-1} \sim \mathbf{167} F_{\text{obs}}(1335)$$

$$F_{\text{int}}(1336) = F_{\text{int}}(1037) \times \Upsilon_{1336}/\Upsilon_{1037}$$

$$1.425 \times 10^{-10} \text{ erg cm}^{-2} \text{ s}^{-1} \text{ \AA}^{-1} \sim \mathbf{200} F_{\text{obs}}(1336)$$



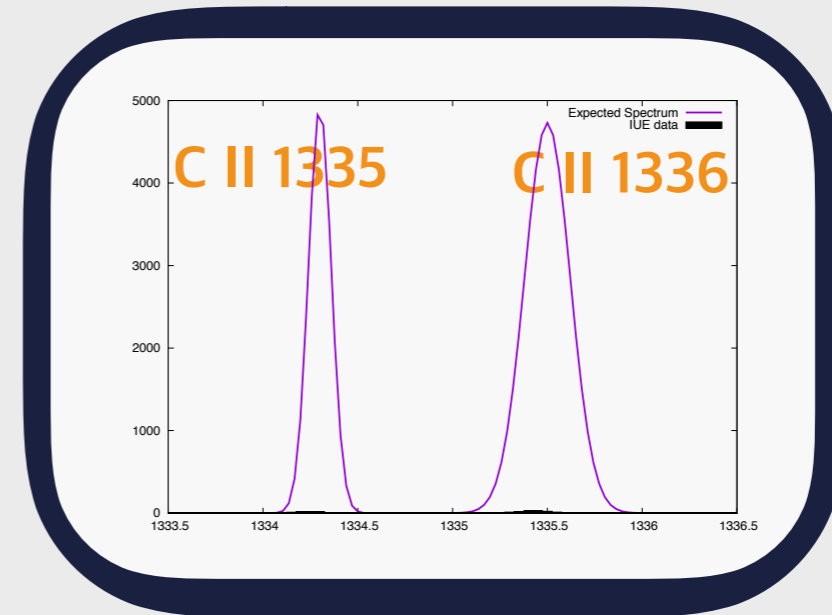
# III. Raman C II and ISM

## ✓ Optical depth of C II emissions

$$\tau = \ln(F_{\text{int}}/F_{\text{obs}})$$

$$\tau(1335) \sim 5.1$$

$$\tau(1336) \sim 5.3$$



★ INTRODUCTION

🔭 OBSERVATION

🖥️ SIMULATION

🍺 DISCUSSION

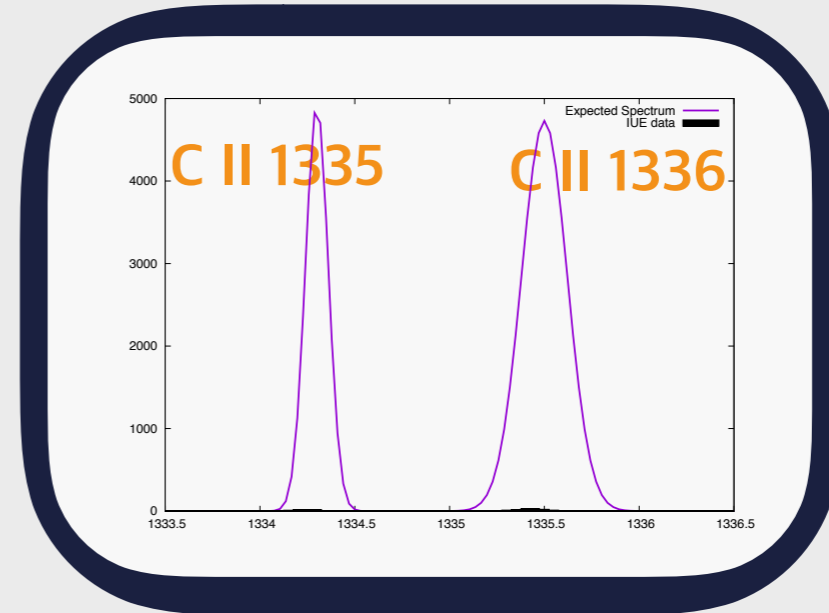
# III. Raman C II and ISM

## ✓ Optical depth of C II emissions

$$\tau = \ln(F_{\text{int}}/F_{\text{obs}})$$

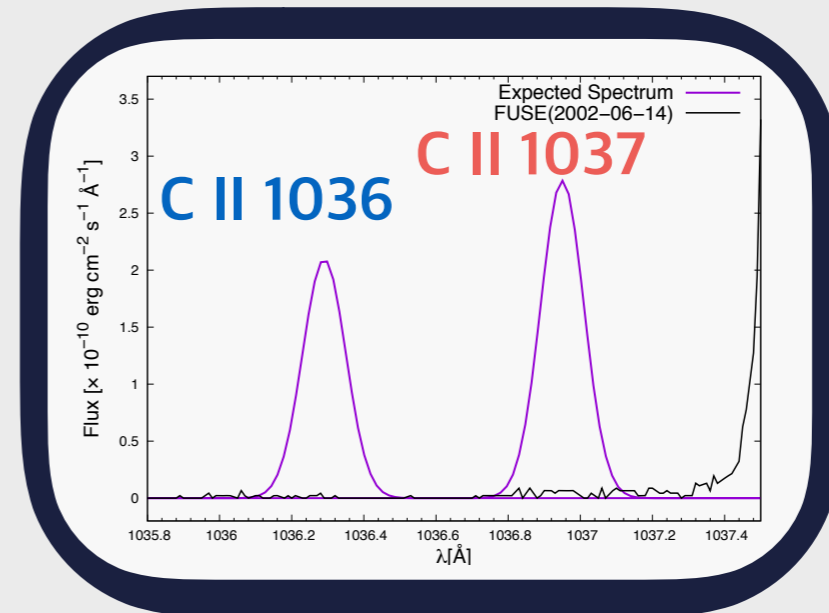
$$\tau(1335) \sim 5.1$$

$$\tau(1336) \sim 5.3$$



$$\tau(1036) \sim 15.81$$

$$\tau(1037) \sim 27.24$$



# III. Raman C II and ISM

★ INTRODUCTION

🔭 OBSERVATION

🖥️ SIMULATION

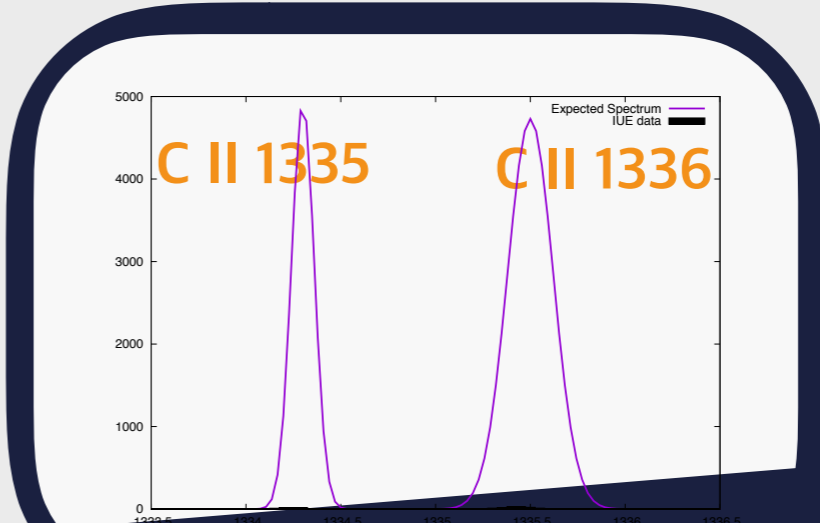
🗣️ DISCUSSION

## ✓ Optical depth of C II emissions

$$\tau = \ln(F_{\text{int}}/F_{\text{obs}})$$

$$\tau(1335) \sim 5.1$$

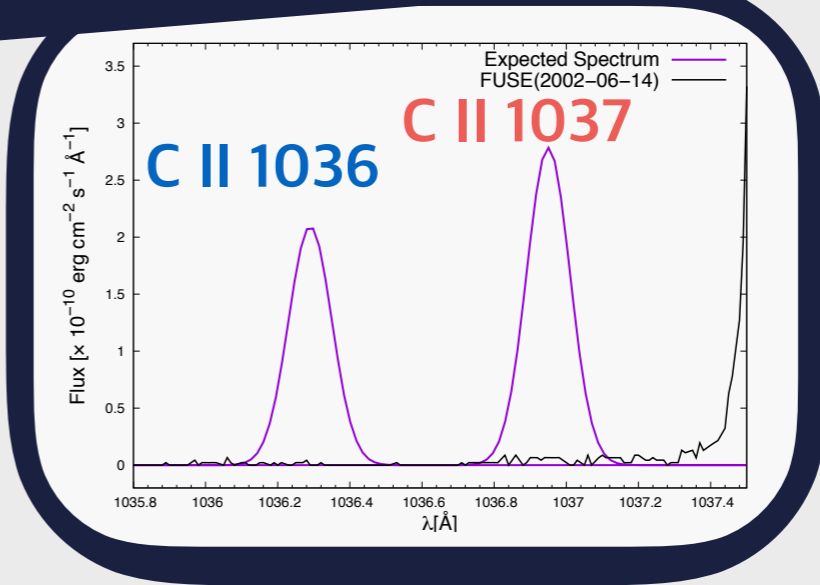
$$\tau(1336) \sim 5.3$$



**Optically thick ISM for C II emissions**

$$\tau(1036) \sim 15.81$$

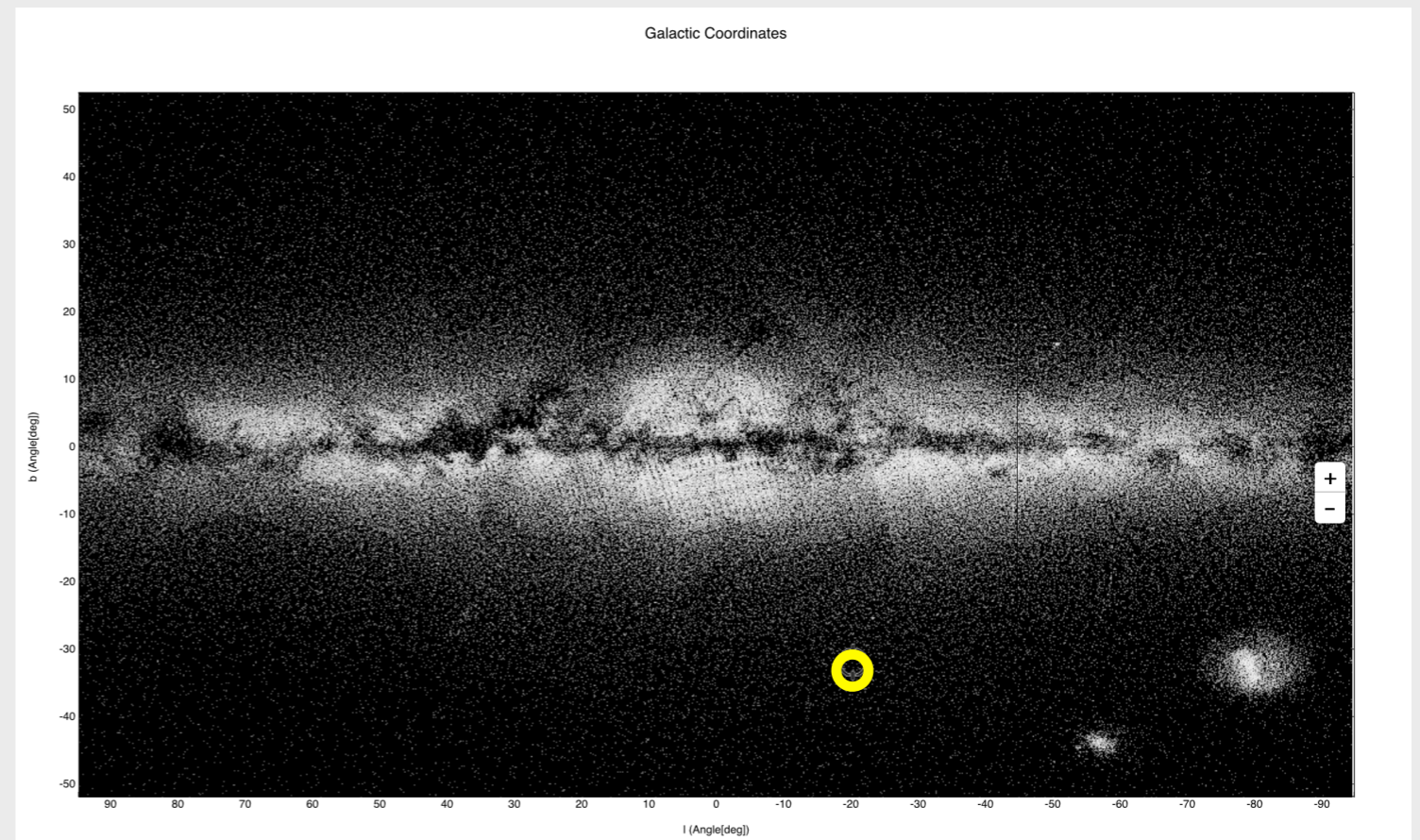
$$\tau(1037) \sim 27.24$$



# III. Raman C II and ISM

## ✓ Extinction of ISM

- Considering a long distance  $d \sim 2.5\text{kpc}$  of RR Tel, it can be originated from the heavy extinction along ISM.
- The column density is expressed by the optical depth and the cross section:  $N(\text{C II}) = \tau / \sigma$
- **$N(\text{CII}) \sim 9.87 \times 10^{13} \text{cm}^{-2}$**



## IV. Summary and Discussion

- ✓ We find two Raman-scattered features of C II at 7023 and 7053 Å in the high-resolution spectrum of the symbiotic nova RR Tel.
- ✓ A significant amount of C II 1036 and 1037 Å emissions are expected, however they are clearly absent in FUSE data.
- ✓ By comparing with other observed C II emissions in IUE data, we conclude that the discrepancy between the observed data and the theoretical expectation is originated from the heavy extinction along ISM.
- ✓ We determine the lower limit of the column density of C II in ISM  $N(\text{CII}) \sim 9.87 \times 10^{13} \text{cm}^{-2}$ .

 INTRODUCTION

 OBSERVATION

 SIMULATION

 DISCUSSION

 THANKS

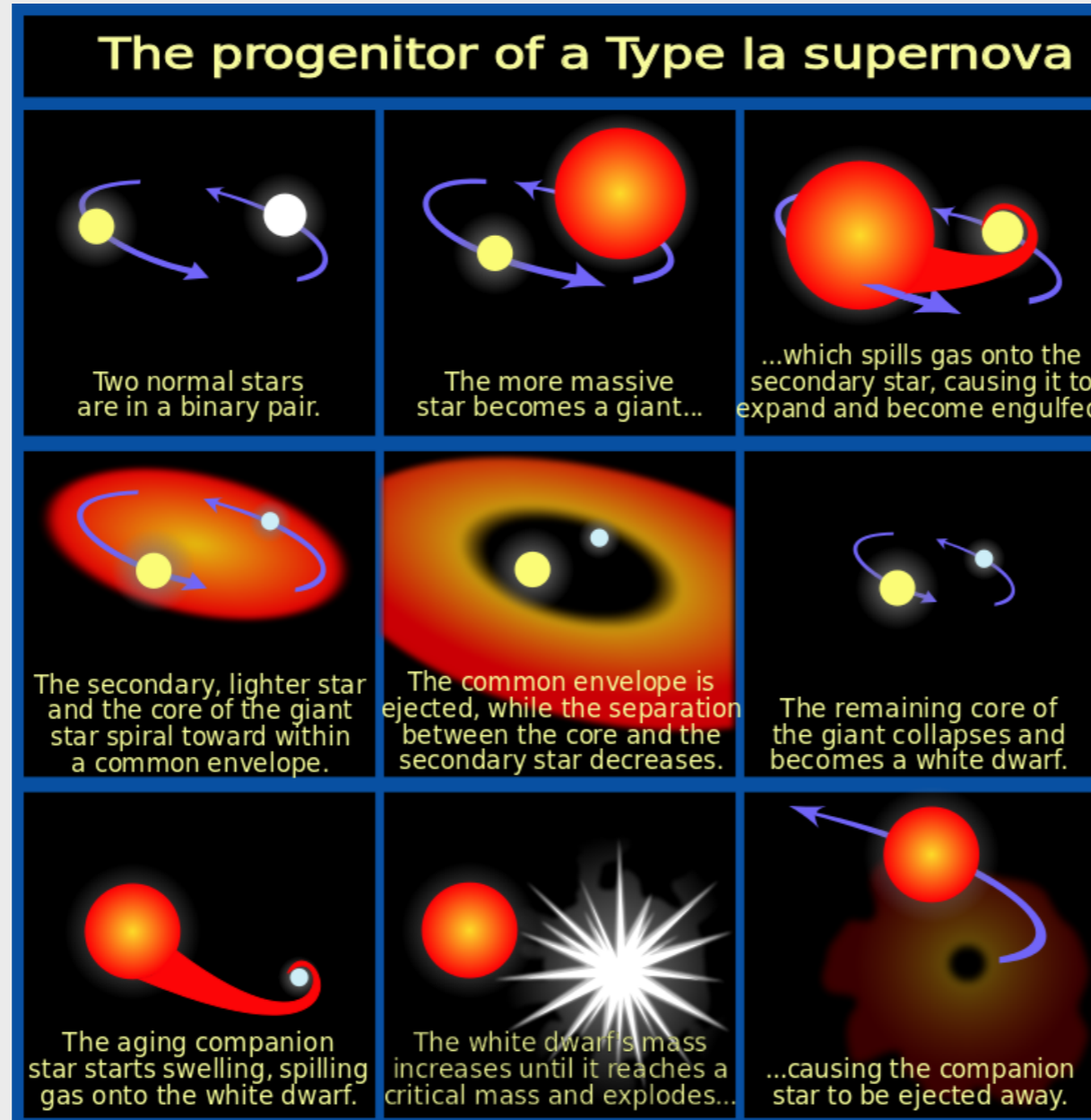
# I. Introduction

★ INTRODUCTION

🔭 OBSERVATION

🖥️ SIMULATION

🍺 DISCUSSION



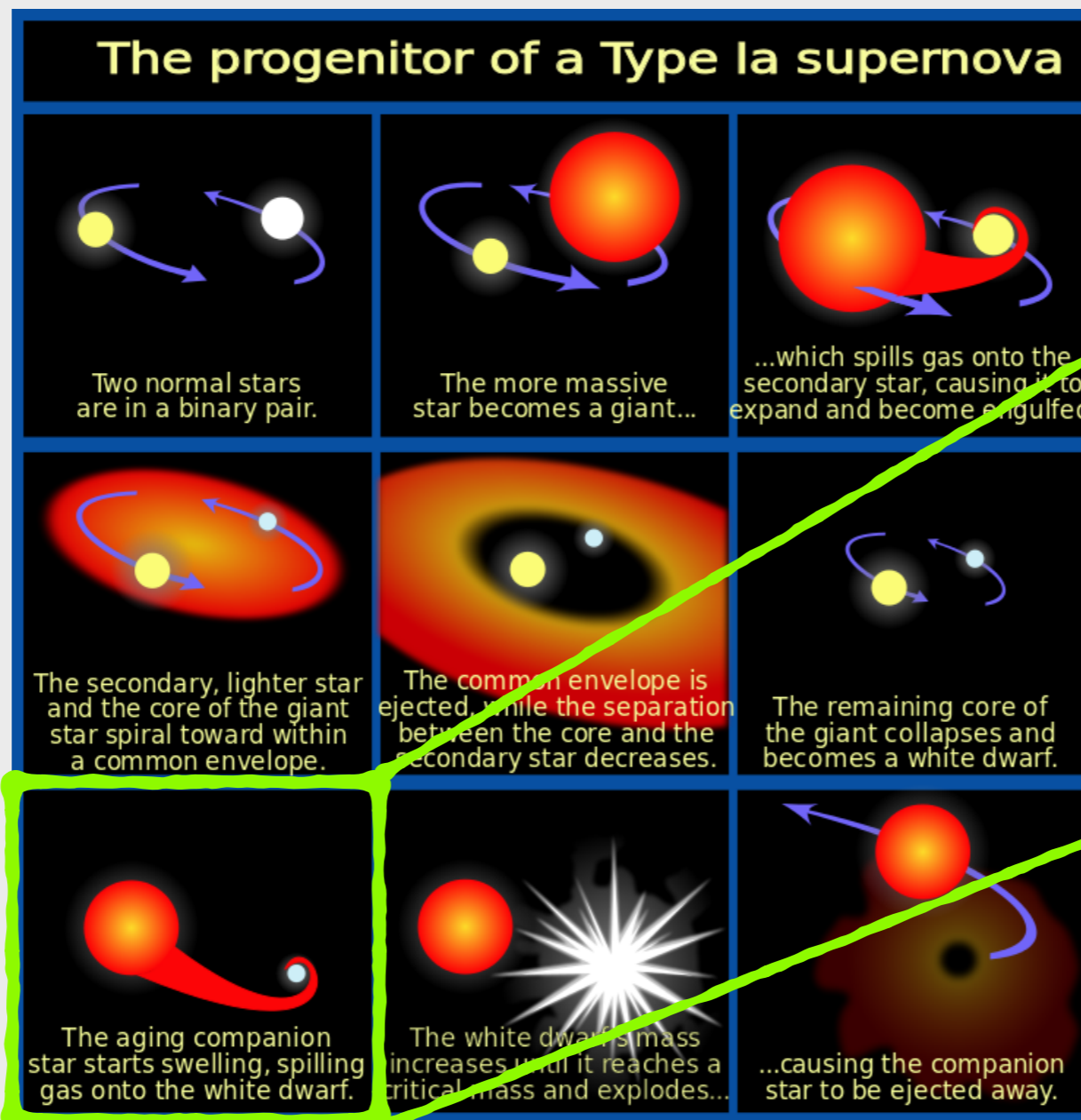
# I. Introduction

★ INTRODUCTION

🔭 OBSERVATION

🖥️ SIMULATION

🍺 DISCUSSION

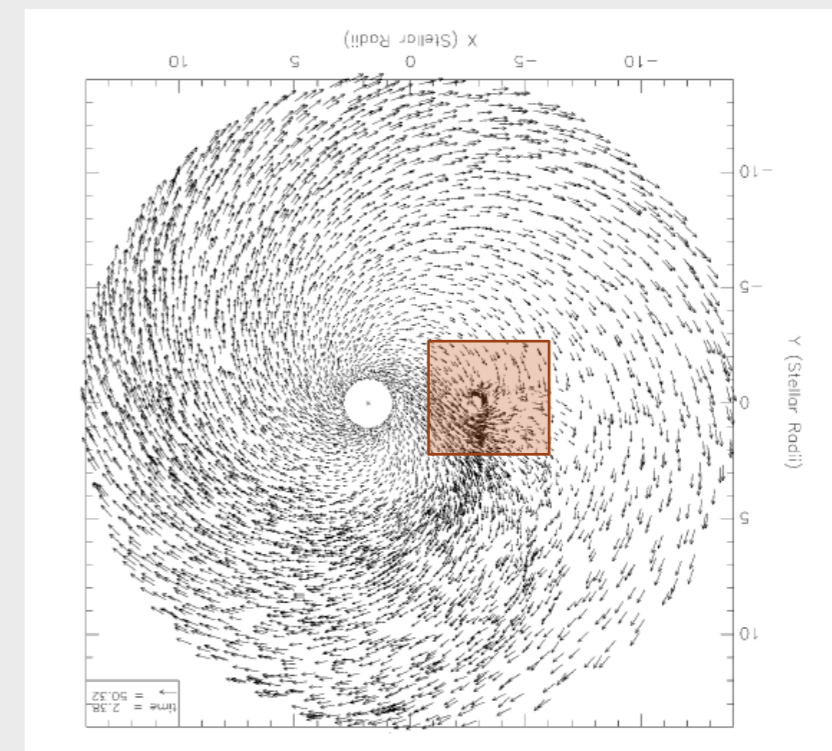
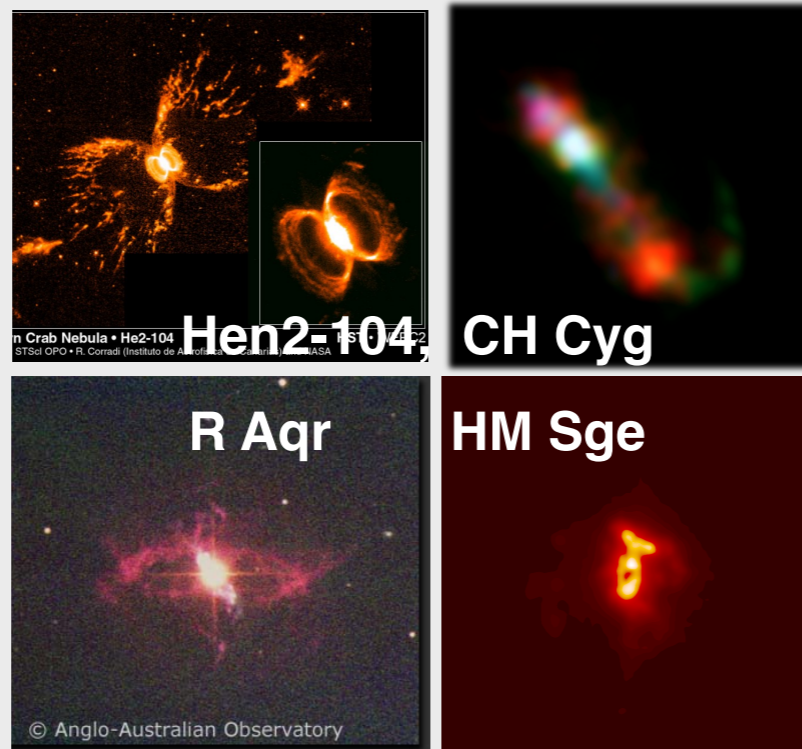




# I. Introduction

## ✓ Symbiotic Stars

- Binary systems consisting of a hot radiation source, usually white dwarf, and a cool, mass losing giant
- A fraction of the slow stellar wind from the giant is gravitationally captured by the white dwarf to presumable form an accretion disk.



SPH Simulation (Mastrodemos and Morris, 1998)

# I. Introduction

## ✓ Raman Scattering

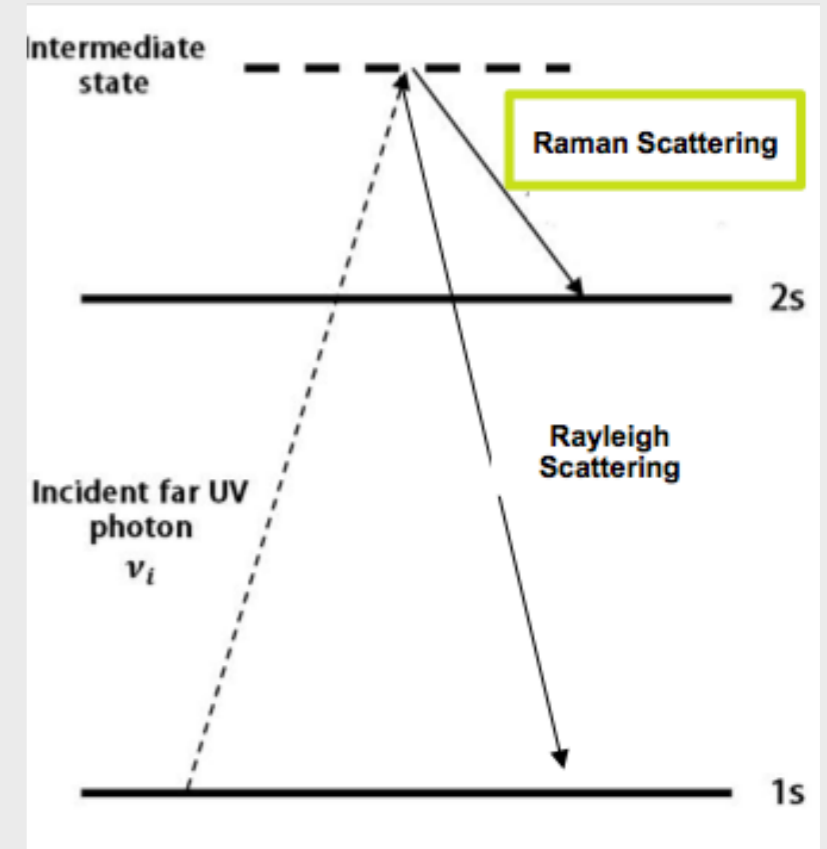
- **A far-UV photon** blueward of Ly $\alpha$  is incident upon a hydrogen atom in the ground state. Subsequently, the hydrogen atom de-excites into the 2s state, **re-emitting an optical Raman-scattered photon.**

- Based on the principle of Energy conservations

$$h\nu_i = h\nu_o + h\nu_\alpha$$

- **The re-emission of a photon has significantly longer wavelength than incident photon.**

$$\lambda_{RV} = \frac{\lambda_{Ly\alpha}\lambda_i}{\lambda_{Ly\alpha} - \lambda_i} \quad (\lambda_{Ly\alpha} = 1215.67\text{\AA})$$



Schematic energy level diagram for Raman-Scattering by H I

Ly  $\beta$  1025 (1s  $\rightarrow$  3p)  $\rightarrow$  H $\alpha$  6563 (3p  $\rightarrow$  2s)

★ INTRODUCTION

🔭 OBSERVATION

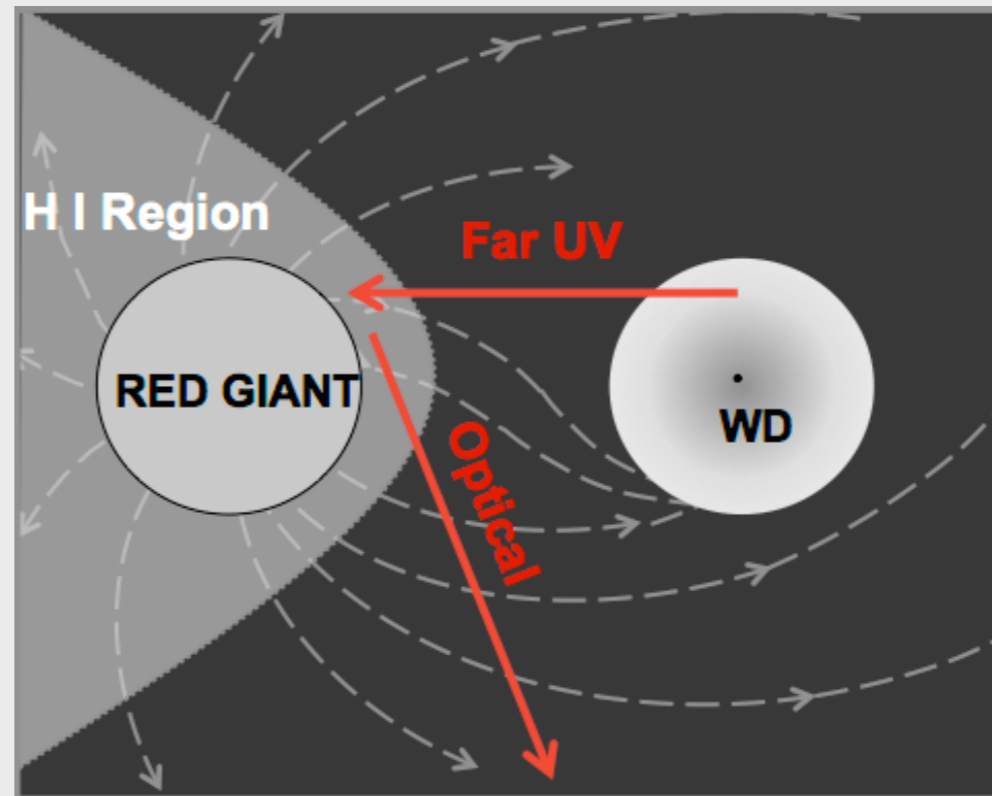
🖥️ SIMULATION

🍺 DISCUSSION

# I. Introduction

## ✓ Raman Scattering in Symbiotic Stars

- The white dwarf accretes a fraction of the stellar wind from the giant, which makes it very hot ( $\sim 10^5$  K) and luminous ( $\sim 10^2 - 10^4 L_{\text{sun}}$ ), and thus capable of ionizing the neutral wind from the giant.



★ INTRODUCTION

🔭 OBSERVATION

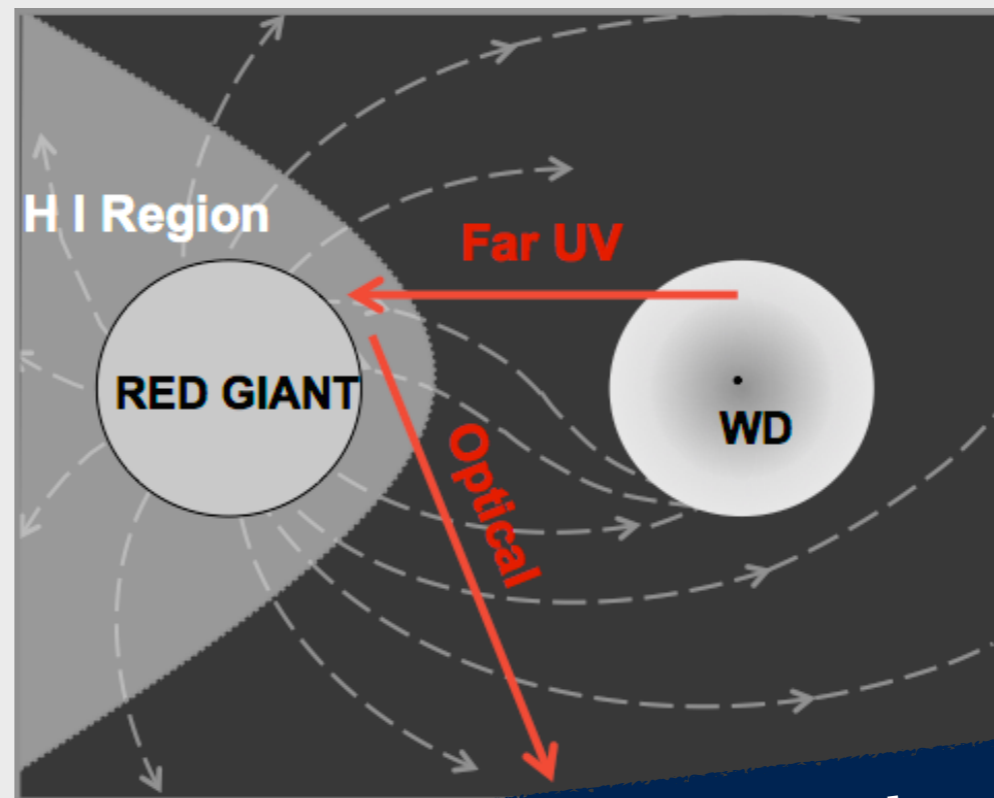
🖥️ SIMULATION

🗣️ DISCUSSION

# I. Introduction

## ✓ Raman Scattering in Symbiotic Stars

- The white dwarf accretes a fraction of the stellar wind from the giant, which makes it very hot ( $\sim 10^5$  K) and luminous ( $\sim 10^2$ - $10^4 L_{\text{sun}}$ ), and thus capable of ionizing the neutral wind from the giant.



**The environment of symbiotic stars is very suitable for observing the Raman-scattering process.**

★ INTRODUCTION

🔭 OBSERVATION

🖥️ SIMULATION

🗣️ DISCUSSION

## II. Observation

### ✓ Raman Lines in RR Tel

- We find seven broad features at 4332, 4850, 6545, 6825, 7025, 7052 and 7082 Å, which are formed through Raman-scattering of He II, C II and O VI by H I.

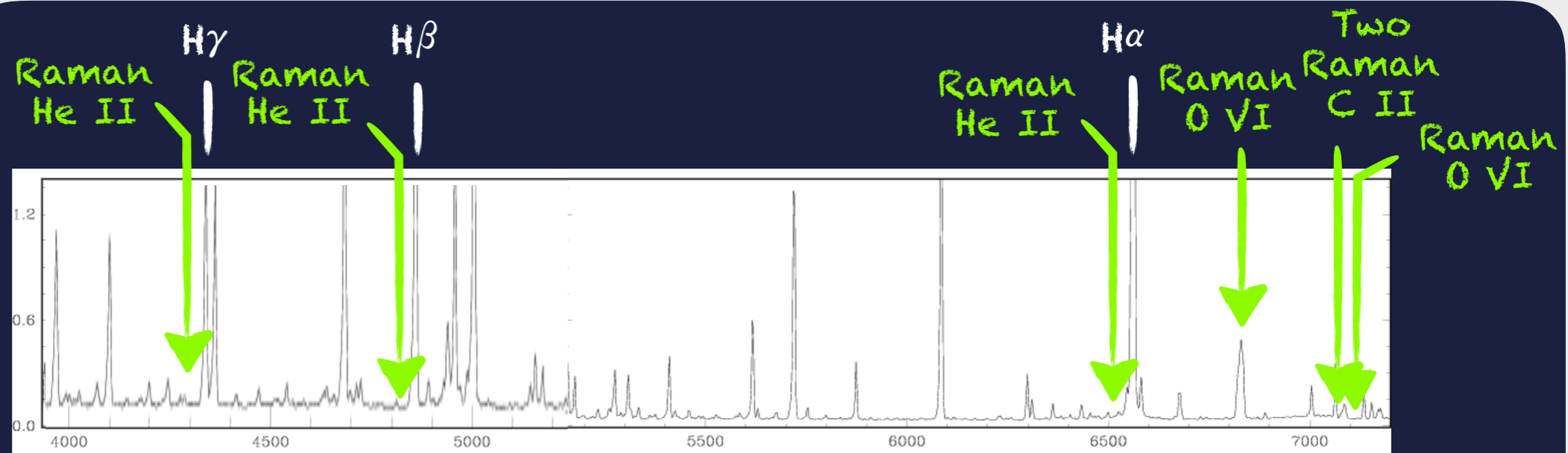


Figure 2. Low-resolution optical spectrum of RR Tel (ESO 1.5m + B&C, Munari & Zwitter, 2002).

Green lines indicate the positions of the observed Raman-scattered lines.

# II. Observation

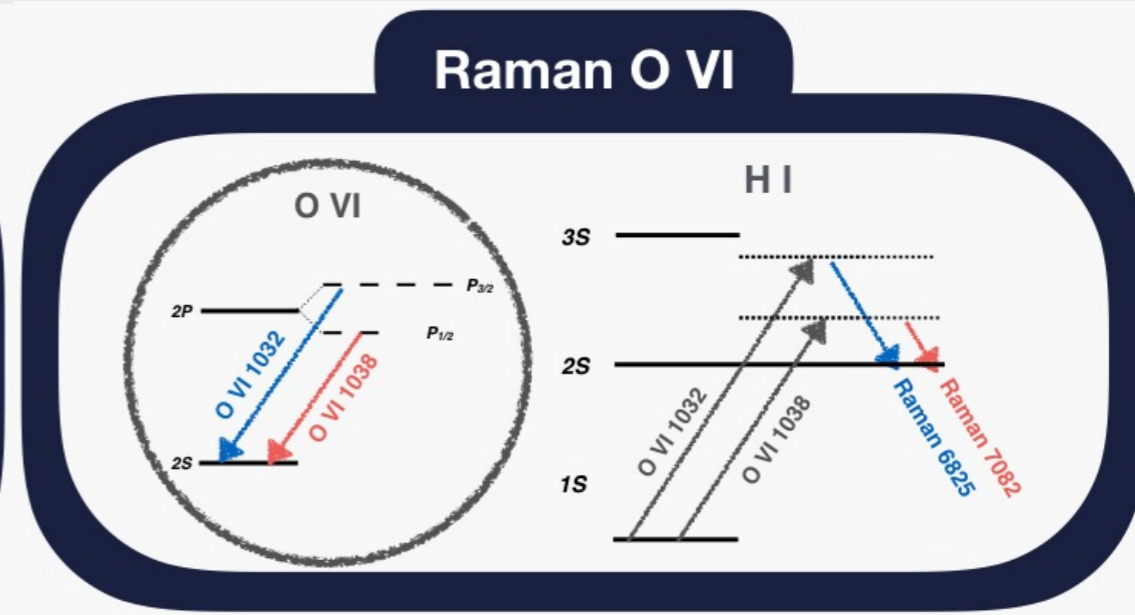
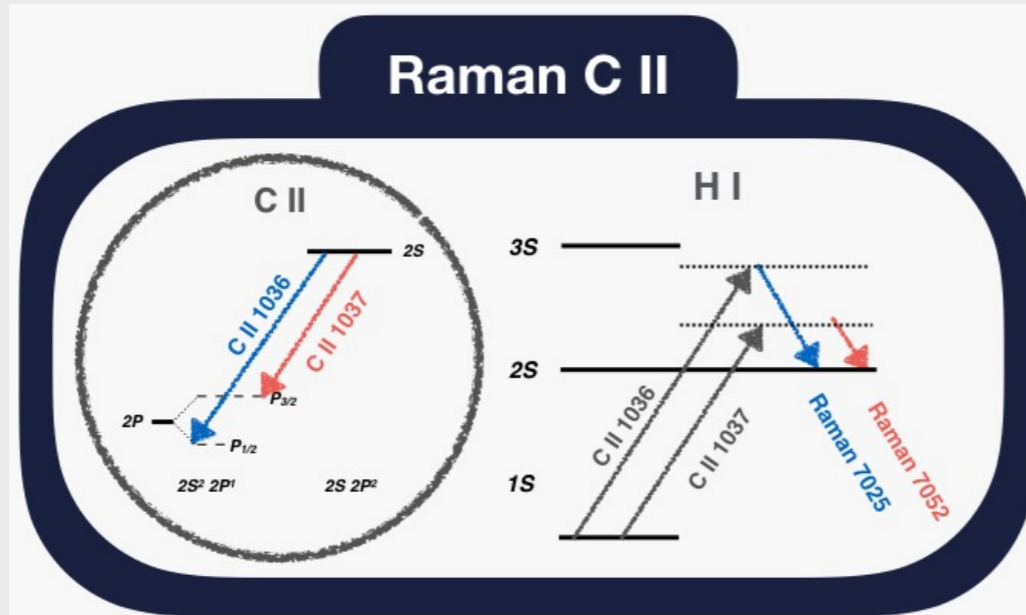
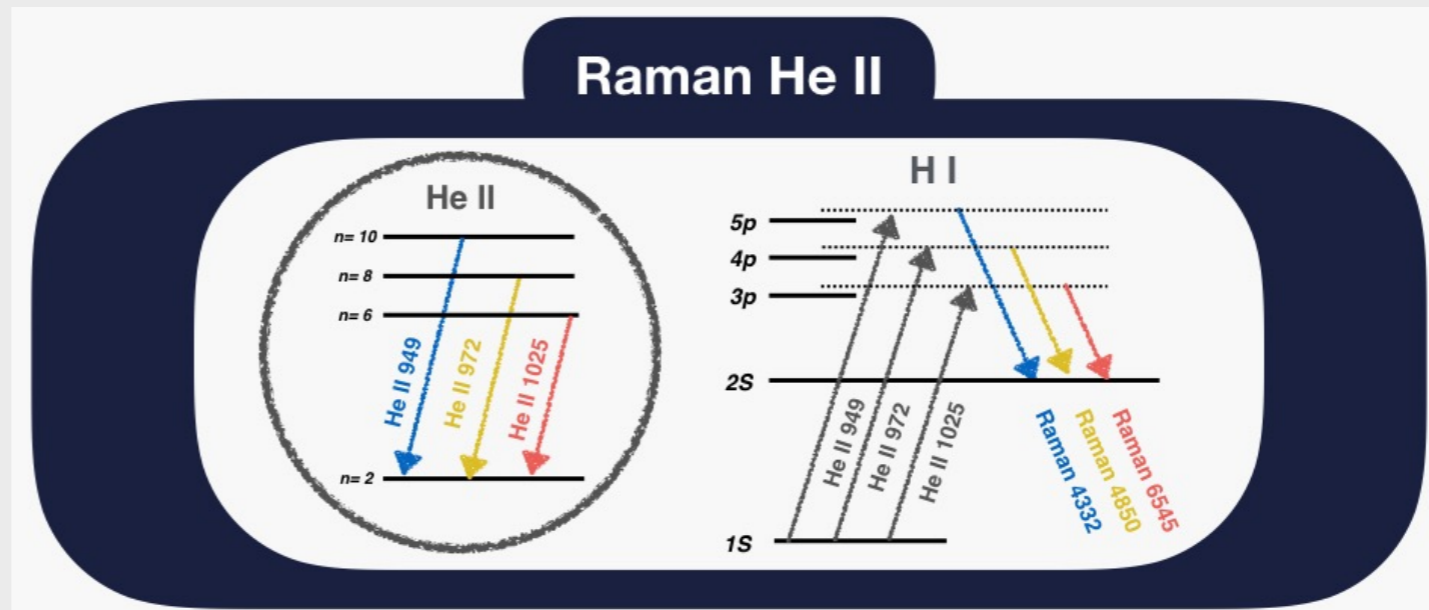
## ✓ Raman Lines in RR Tel

★ INTRODUCTION

🔭 OBSERVATION

🖥️ SIMULATION

🗣️ DISCUSSION



# II. Observation

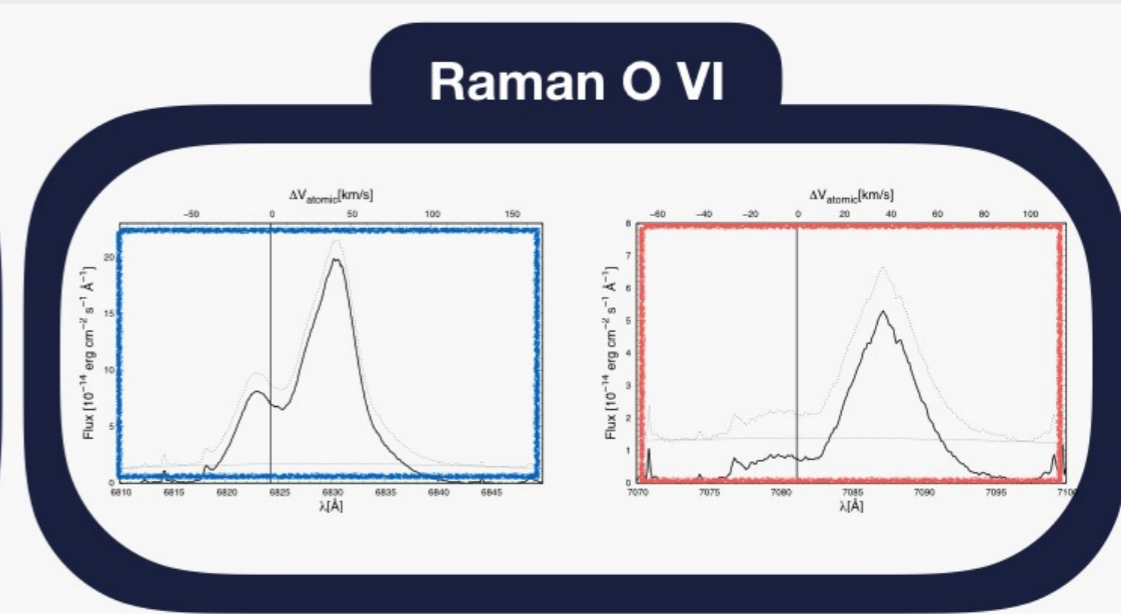
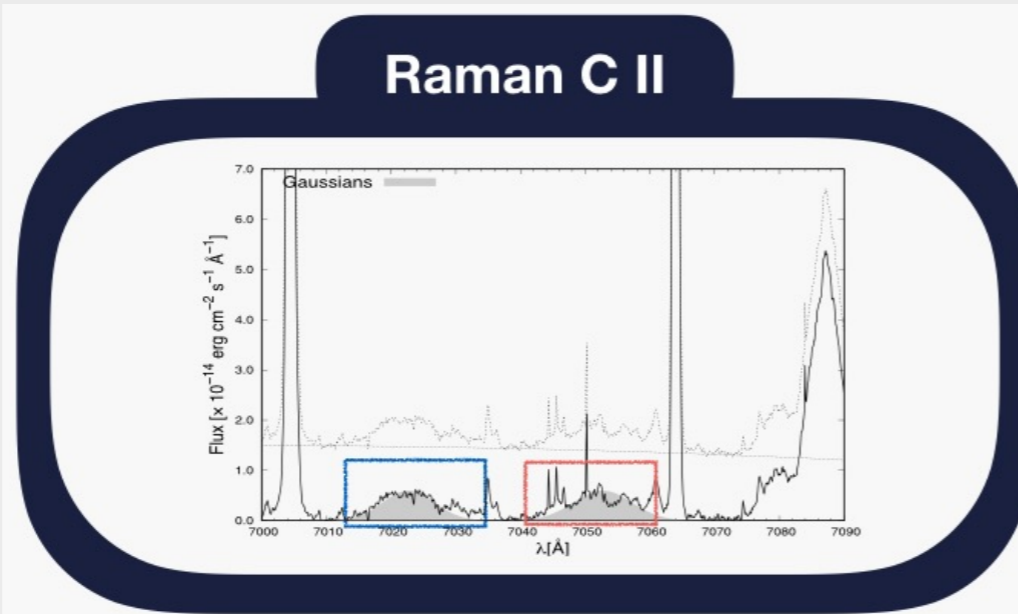
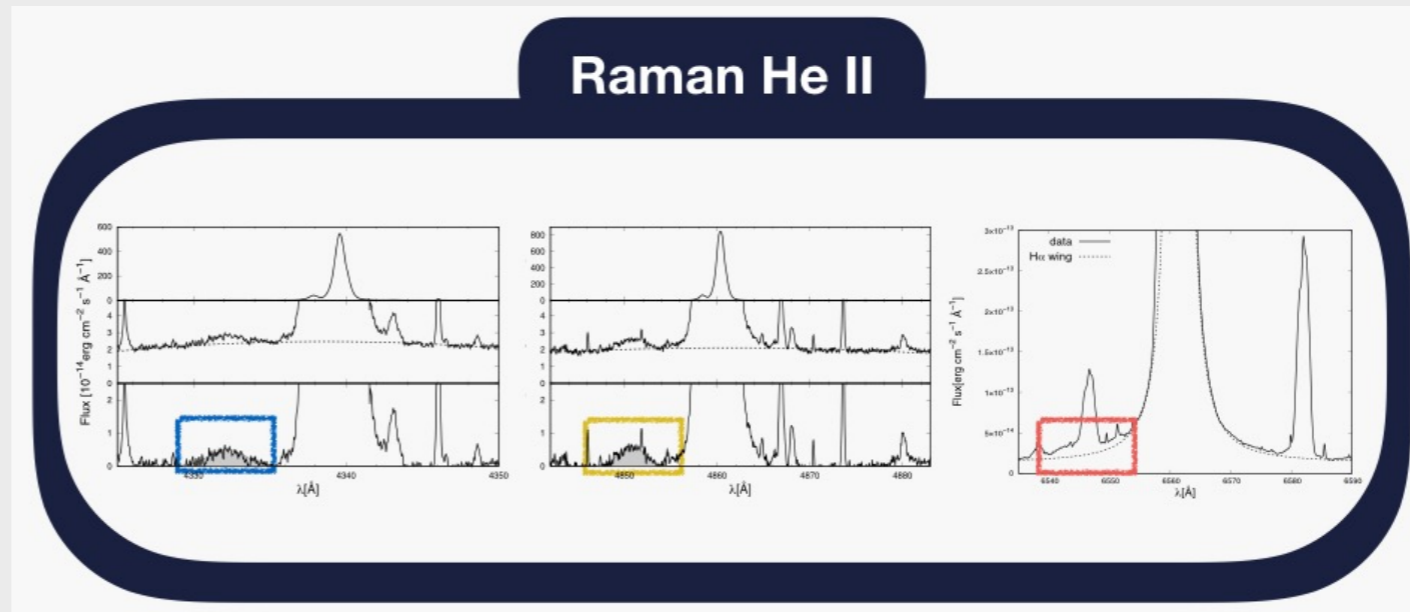
## ✓ Raman Lines in RR Tel

★ INTRODUCTION

🔭 OBSERVATION

🖥️ SIMULATION

🗨️ DISCUSSION



# III. Monte Carlo Simulations

## ✓ STB ionization front

- In STB (Seaquist, Taylor & Button, 1984) model, the ionization front in the stellar wind region around the giant is determined by the balance of photoionization by the H-ionizing flux from the hot component and recombination represented by the mass loss rate of the giant.
- A parameter  $X$  in STB geometry is given by  $X = 4\pi a L_H / \alpha_B (m_H v_\infty / \dot{M})^2$ .

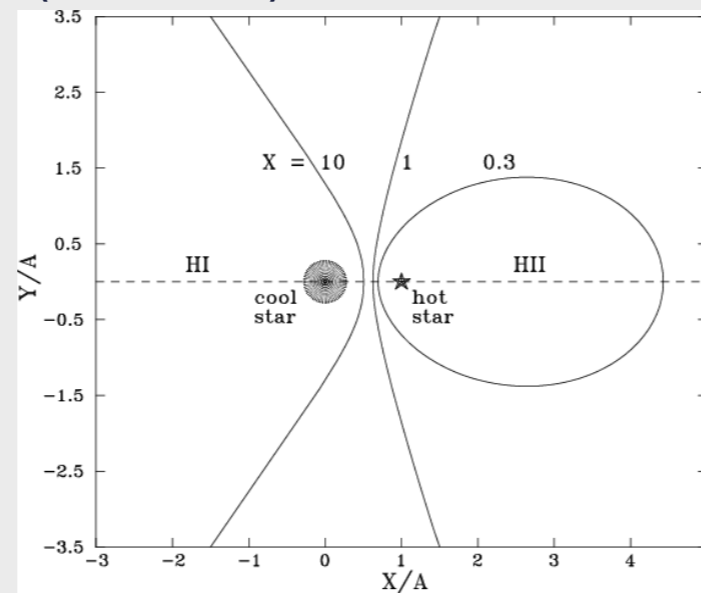


Figure 4. An ionization structure with STB Geometry (left)



# III. Raman C II and ISM

## ✓ C II 1335 Triplet

Table 4. C II emissions

Transition		$\lambda$	$\Upsilon^a$	$A_L^b$	$F_{obs}$	$F_{int}$
$2s^22p$	$2s2p^2$	(Å)	$T = 10^4\text{K}$	( $s^{-1}$ )	( $\text{erg cm}^{-2} \text{s}^{-1}$ )	( $\text{erg cm}^{-2} \text{s}^{-1}$ )
$^2P_{1/2}^0$	$^2S_{1/2}$	1036.34	0.608	$7.971 \times 10^8$	...	$3.15 \times 10^{-11}$
$^2P_{2/3}^0$	$^2S_{1/2}$	1037.02	1.222	$1.575 \times 10^9$	...	$4.19 \times 10^{-11}$
$^2P_{1/2}^0$	$^2D_{3/2}$	1334.53	1.431	$2.567 \times 10^8$	$4.43 \times 10^{-13}$	$7.41 \times 10^{-11}$
$^2P_{2/3}^0$	$^2D_{3/2}$	1335.66	1.058	$5.08 \times 10^7$	$7.15 \times 10^{-13}$	$1.425 \times 10^{-10}$
$^2P_{2/3}^0$	$^2D_{5/2}$	1335.71	3.098	$3.067 \times 10^8$		

<sup>a</sup>Tayal 2008

<sup>b</sup>NIST database

★ INTRODUCTION

🔭 OBSERVATION

🖥️ SIMULATION

🍺 DISCUSSION

# III. Monte Carlo Simulations

## ✓ Hierarchical Emission Region Model

- In order to reproduce the Raman-scattered line profiles, we suggest that the emission nebulae around the white dwarf has a hierarchical structure including inner most part with **O VI disk** and the outer part with **C II** and **He II sphere**, which is consistent with the higher ionization potential of O VI than those of He II and C II.

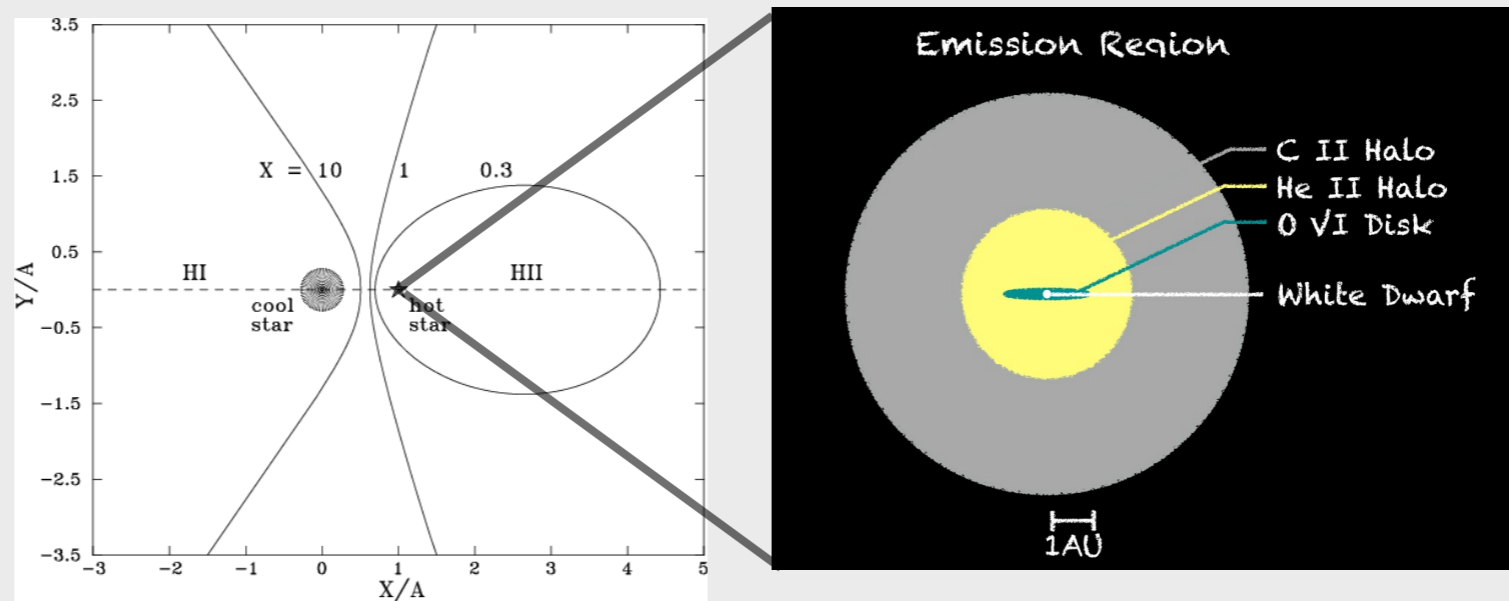


Figure 4. An ionization structure with STB Geometry (left) and schematic model for the emission nebula around the WD (right)

# III. Monte Carlo Simulations

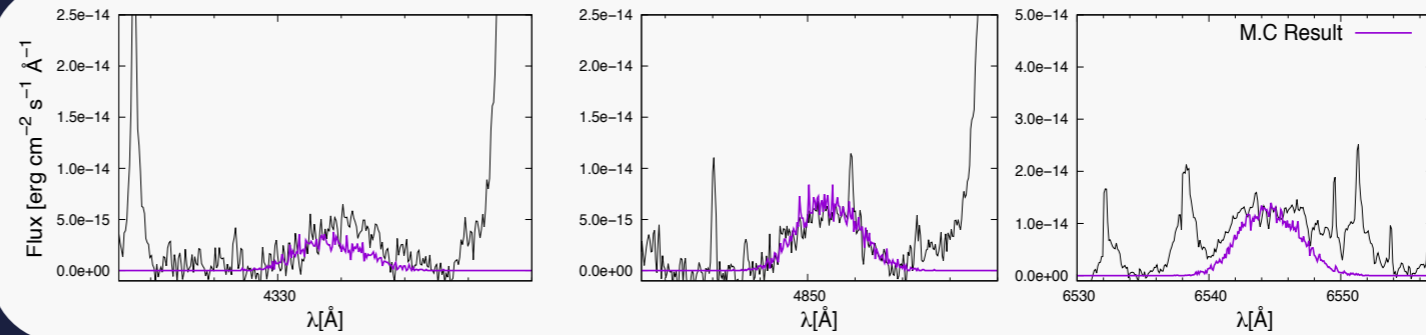
★ INTRODUCTION

🔭 OBSERVATION

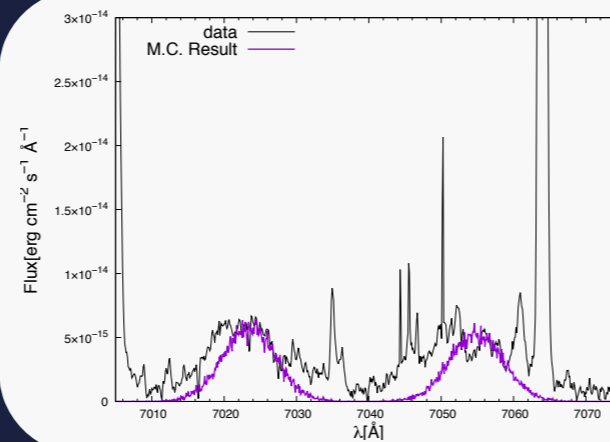
🖥️ SIMULATION

🍻 DISCUSSION

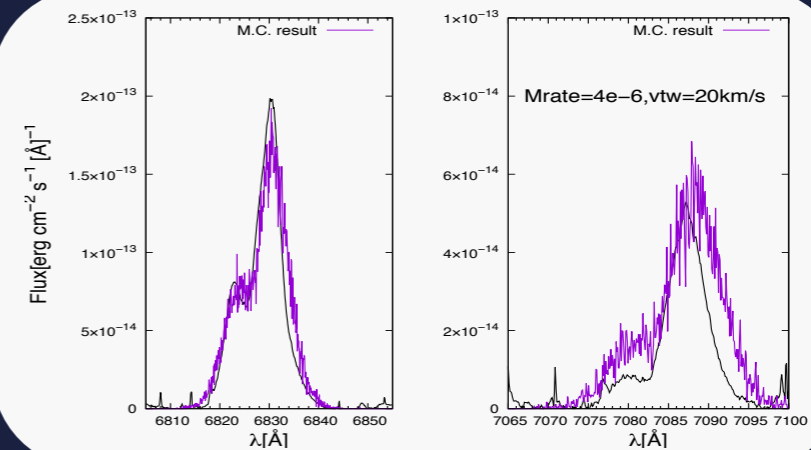
## Raman He II



## Raman C II



## Raman O VI



- A good fit is obtained for the mass loss rate  $\dot{M} \sim 3 \times 10^{-6} M_{\odot}/\text{yr}$  and  $v_{\infty} = 10 \text{ km/s}$ , which corresponds to  $X \sim 7.5$ .
- Raman lines are well fitted with hierarchical emission region composed of the O VI disk extending 1AU and the He II and C II spheres with a size of sub AU.

# III. Monte Carlo Simulations

## ✓ STB ionization front

- In STB (Seaquist, Taylor & Button, 1984) model, the ionization front in the stellar wind region around the giant is determined by the balance of photoionization by the H-ionizing flux from the hot component and recombination represented by the mass loss rate of the giant.
- A parameter  $X$  in STB geometry is given by  $X = 4\pi a L_H / \alpha_B (m_H v_\infty / \dot{M})^2$ .

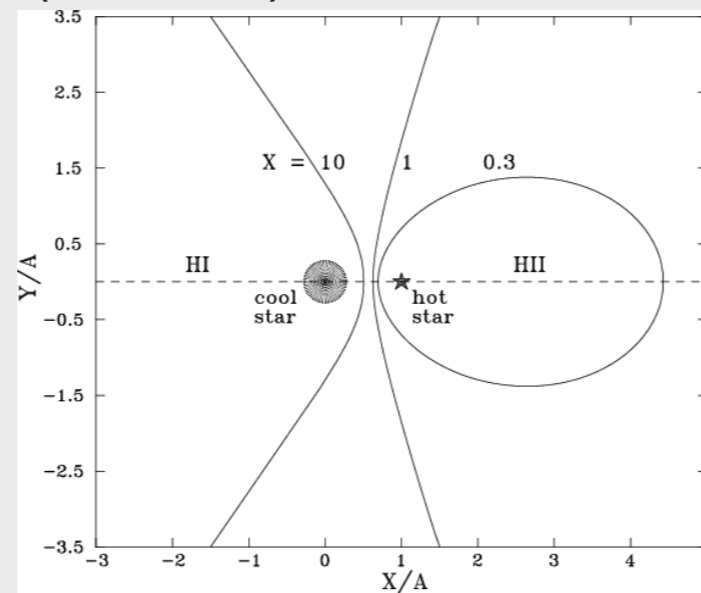


Figure 4. An ionization structure with STB Geometry (left)